genetic model for myelin-related axonopathy. J Neurosci 2003; 23: 2833–9.

Sidman RL, Angevine JB, Pierce ET. Atlas of mouse brain and spinal cord. Cambridge: Harvard University Press; 1971.

Sung JH, Mastri AR, Park SH. Axonal dystrophy in the gracile nucleus in children and young adults. J Neuropathol Exp Neurol 1981; 40: 37–45.

Takahashi T, Yagishita S, Amano N, Yamaoka K, Kamei T. Amyotrophic lateral sclerosis with numerous axonal spheroids in the corticospinal tract and massive degeneration of the cortex. Acta Neuropathol (Berl) 1997; 94: 294–9.

Trapp BD, Peterson J, Ransohoff RM, Rudick R, Mork S, Bo L. Axonal transection in the lesions of multiple sclerosis. N Engl J Med 1998; 338: 278–85.

Tu PH, Raju P, Robinson KA, Gurney ME, Trojanowski JQ, Lee VM. Transgenic mice carrying a human mutant superoxide dismutase transgene develop neuronal cytoskeletal pathology resembling human amyotrophic lateral sclerosis lesions. Proc Natl Acad Sci USA 1996; 93: 3155–60.

van Leeuwen FW, de Kleijn DP, van den Hurk HH, Neubauer A, Sonnemans MA, Sluijs JA, et al. Frameshift mutants of beta amyloid precursor protein and ubiquitin-B in Alzheimer's and Down patients. Science 1998; 279: 242–7.

Wang MS, Davis AA, Culver DG, Glass JD. Wld^S mice are resistant to paclitaxel (Taxol) neuropathy. Ann Neurol 2002; 52: 442–7.

Wilson SM, Bhattacharyya B, Rachel RA, Coppola V, Tessarollo L, Householder DB, et al. Synaptic defects in ataxia mice result from a mutation in Usp14, encoding a ubiquitin-specific protease. Nat Genet 2002; 32: 420–5.

Wujek JR, Lasek RJ. Correlation of axonal regeneration and slow component B in two branches of a single axon. J Neurosci 1983; 3: 243–51.

Yamazaki K, Wakasugi N, Tomita T, Kikuchi T, Mukoyama M, Ando K. Gracile axonal dystrophy (gad), a new neurological mutant in the mouse. Proc Soc Exp Biol Med 1988; 187: 209–15.

Zhai Q, Wang J, Kim A, Liu Q, Watts R, Hoopfer E, et al. Involvement of the ubiquitin–proteasome system in the early stages of Wallerian degeneration. Neuron 2003; 39: 217–25.

Journal of Neurochemistry, 2005, **92**, 1061–1072 doi:10.1111/j.1471-4159.2004.02963.x

Potentiation of ATP-induced currents due to the activation of P2X receptors by ubiquitin carboxy-terminal hydrolase L1

Yoshimasa Manago,* Yoshiko Kanahori,* Aki Shimada,* Ayumi Sato,* Taiju Amano,* Yae Sato-Sano,*'† Rieko Setsuie,*'† Mikako Sakurai,*'† Shunsuke Aoki,† Yu-Lai Wang,† Hitoshi Osaka,†'‡ Keiji Wada† and Mami Noda‡

**Laboratory of Pathophysiology, Graduate School of Pharmaceutical Sciences, Kyushu University, Fukuoka, Japan*

†Department of Degenerative Neurological Diseases, National Institute of Neuroscience, National Center of Neurology and Psychiatry, Tokyo, Japan

‡Information and Cellular function, PRESTO, Japan Science and Technology Corporation (JST), Kawaguchi, Saitama, Japan

Abstract

Mammalian neuronal cells abundantly express a de-ubiquitinating isozyme, ubiquitin carboxy-terminal hydrolase L1 (UCH L1). Loss of UCH L1 function causes dying-back type of axonal degeneration. However, the function of UCH L1 in neuronal cells remains elusive. Here we show that overexpression of UCH L1 potentiated ATP-induced currents due to the activation of P2X receptors that are widely distributed in the brain and involved in various biological activities including neurosecretion. ATP-induced inward currents were measured in mock-, wild-type or mutant (C90S)-UCH L1-transfected PC12 cells under the conventional whole-cell patch clamp configuration. The amplitude of ATP-induced currents was significantly greater in both wild-type and C90S UCH L1-transfected cells, suggesting that hydrolase activity was not involved but increased level of mono-ubiquitin might play an important role. The increased currents were dependent on cAMP-dependent protein kinase (PKA) and Ca^{2+} and calmodulin-dependent protein kinase (CaMKII) but not protein kinase C. In addition, ATP-induced currents were likely to be modified via dopamine and cyclic AMP-regulated phosphoprotein (DARPP-32) that is regulated by PKA and phosphatases. Our finding shows the first evidence that there is a relationship between UCH L1 and neurotransmitter receptor, suggesting that UCH L1 may play an important role in synaptic activity.

Keywords: CaMKII, DARPP-32, PKA, patch-clamp, PC12, UCH L1.

J. Neurochem. (2005) **92**, 1061–1072.

The ubiquitin-proteasome system is an evolutionarily conserved and energy-dependent proteolytic pathway that functions constitutively to degrade proteins. Recent studies indicate that ubiquitin-mediated proteolysis can also be regulated and is of widespread importance (Wilkinson 1995; Coux *et al.* 1996). Regulated proteolysis by the ubiquitin-

Received August 24, 2004; accepted October 8, 2004.

Address correspondence and reprint requests to Mami Noda, PhD, Laboratory of Pathophysiology, Graduate School of Pharmaceutical Sciences Kyushu University, 3-1-1 Maidashi, Higashi-ku, Fukuoka 812–8582, Japan, Tel./Fax: + 81-92-642-6574.
E-mail: noda@phar.kyushu-u.ac.jp

Abbreviations used: ATP, adenosine triphosphate; BSA, bovine serum albumin; CaMKII, Ca^{2+} and calmodulin-dependent protein kinase; CDK, cyclin-dependent kinase; CHO, cells, Chinese hamster ovary cells; CREB, Ca^{2+}-stimulated cAMP response element binding protein; DAPI, 4′, 6-diamidino-2-phenylindole, dihydrochloride; EGTA, ethyleneglycol-bis-N, N, N′, N′-tetraacetic acid; ERK, extracellular signal-regulated kinase; DARPP-32, dopamine and cyclic AMP-regulated phosphoprotein with molecular weight of about 32 000; 1,9-dideoxyforskolin, 7β-acetoxy-6β-hydroxy-8,13-epoxy-labd-14-en-11-one; FBS, fetal bovine serum; forskolin, 7β-acetoxy-8,13-epoxy-1α,6β,9α-trihydroxy-labd-14-en-11-one; H-89, N-[2-(p-bromoocinamylamino)ethyl]-5-isoquinolinesulfonamide; HS, horse serum; KN-93, 2-[N-(2-hydroxyethyl)]-N-(4-methoxybenzenesulfonyl)]amino-N-(4-chlorocinnamyl)-N-methylbenzylamine); HEPES, N-2-hydroxyethylpiperazine-N′-2-ethansulfonic acid; MAPK, mitogen-activated protein kinase; NGF, nerve growth factor; PBS(–), Dulbecco's Ca^{2+}, Mg^{2+}-free phosphate buffer saline; PC12, cells, rat phenochromocytoma cells; PD98059, 2′-Amino-3′-methoxyflavone; PGP9.5, protein gene product 9.5; PKA, cyclic AMP-dependent protein kinase; PKC, protein kinase C; PP1, protein phosphatase 1; PP2, protein phosphatase 2; SDS-PAGE, sodium dodecyl sulfate-polyacrylamide gel electrophoresis; TBST, Tris buffer saline-Tween; Thr-34, threonine at 34; Thr-75, threonine at 75; Roscovitine, 2-(R)-(1-Ethyl-2-hydroxyethylamino)-6-benzylamino-9-isopropylpurine; UCH, L1, ubiquitin C-terminal hydrolase L1.

proteasome pathway has been implicated in the control of cell cycle (King *et al.* 1996), transcription activation (Verma *et al.* 1995), antigen presentation (Rock *et al.* 1994), cell fate and growth (Huang *et al.* 1995; Zhu *et al.* 1996), synaptogenesis (Muralidhar and Thomas 1993; Oh *et al.* 1994) and memory (Hegde *et al.* 1997). Ubiquitination of proteins is mediated by specific enzymes (E1, E2, and E3) and polyubiquitinated proteins are translocated to the 26S proteasome and subsequently proteolytically degraded (Ciechanover *et al.* 2000). Conversely, deubiquitination is thought to be essential for the regulation of proteolysis and for recycling of monoubiquitin from polyubiquitin chains.

Recently, one of the deubiquitinating enzymes, UCH L1 (ubiquitin carboxy-terminal hydrolase L1), was reported to be essential for brain function. UCH L1 is selectively expressed in neuron and testis (Wilkinson *et al.* 1989; Wilkinson *et al.* 1992). Loss of UCH L1 function was shown to cause neuronal degeneration observed in the gracile axonal dystrophy (*gad*) mouse (Saigoh *et al.* 1999), and missence mutation of UCH L1 was found in familial Parkinson disease (Leroy *et al.* 1998). As physiological functions of UCH L1, it is not limited to hydrolase activity; it has been shown that it associated with mono-ubiquitin and thus stabilized free ubiquitin by preventing its degradation within lysosomes. UCH L1's affinity for ubiquitin rather than hydrolase activity was required for the regulation of ubiquitin level (Osaka *et al.* 2003) and UCH L1 even might work as ubiquitin ligase (Liu *et al.* 2002). Furthermore, UCH L1 has been reported to have an important role in apoptosis in germ cell and neuron (Harada *et al.* 2004; Kwon *et al.* 2004b) and different UCH isozymes have distinct function during spermatogenesis (Kwon *et al.* 2004a).

As for neural function of UCH L1, little is known yet. In *Aplysia*, homologous UCH was shown to be important for learning and memory (Hegde *et al.* 1997). It is not yet known that UCH L1 works in a similar way in mammalian cells, but these results strongly suggest that UCH L1 plays an important role in synaptic function and morphology. In the present study, we investigated the neuronal function of UCH L1 on receptor channels which affect neurotransmitter secretion.

PC12 cells are often used as a model for studying neuronal cell function. Among neurotransmitter receptors expressed in PC12 cells, ATP receptors induce dopamine release (Sela *et al.* 1991). ATP receptors are divided into two subtypes, P2X and P2Y receptors. P2X receptors are ionotropic receptors and form cationic channels, while P2Y receptors are G-protein-coupled receptors and $P2Y_{1,\ 2,\ 4,\ 6,\ 11}$ cause intracellular Ca^{2+} mobilization via IP3 formation and activate Ca^{2+}-dependent K^+ channels (Ikeuchi *et al.* 1996). Among P2X receptors, $P2X_2$ and $P2X_4$ receptor mRNA have been detected in PC 12 cells (Hur *et al.* 2001). P2X receptors mediate fast ionic flow and are supposed to induce depolarization of the cells, hence contributing to the catecholamine release from PC12 cells. Therefore, we first analyzed P2X receptors and their modulation by UCH L1. This is the first report to show a relationship between UCH L1 and neurotransmitter receptors and may help to understand the function of UCH L1 in the nervous system.

Materials and methods

Cell culture

PC12 Tet-off cells were grown in RPMI-1640 medium containing 5% fetal bovine serum (FBS) (Cell Culture Technologies, CANSER INTERNATIONAL INC., Canada), 10% horse serum (HS) (Gibco/BRL, Grand Island, NY, USA), 100 units/mL penicillin (Life Technologies, Rockville, MD, USA) and 100 μg/mL streptomycin (Life Technologies) in a humidified atmosphere with 10% CO_2 at 37°C. To differentiate PC12 Tet-off cells, 100 ng/mL of nerve growth factor (NGF) was added to the RPM1640 medium with 0.1% HS, 0.05% FBS, 50 unit/mL penicillin and 100 μg/mL streptomycin for 4 days.

CHO-AA8-Lucl cells were maintained in Minimum Essential Medium Eagle α modification (Sigma, St Louis, MO, USA) containing 10% FBS, 100 units/mL penicillin, 100 μg/mL streptomycin, and 4 mM L-glutamine (Gibco/BRL), with 10% CO_2 at 37°C.

Transfection

Plasmids used for transfection were constructed using pBI-EGFP Tet vector (Clontech). For electrophysiological recording, PC12 Tet-Off cells were transfected with mock, wild-type or mutant (C90S) human UCH L1 cDNA, using Lipofectamine 2000. After 24 h, PC12 Tet-Off cells were treated with NGF and differentiated for 4–5 days. More precisely, $3.0 \times \sim 10^5$/dish PC12 Tet-Off cells were seeded in 35-mm dishes in RPMI with 10% HS and 5% FBS. Twenty-four hours after seeding, the medium was replaced with 500 μL of serum-free RPMI1640 medium. Then, the transfection mixture containing 4 μg of cDNA and 10 μL of Lipofectamine 2000 in 500 μL of RPMI-1640 was added to each dish and incubated for 6 h in a humidified atmosphere with 10% CO_2 at 37°C. One ml of complete RPMI-1640 supplemented with an additional 10% HS and 5% FBS was then added to each dish. The solution for transfection was discarded 18 h later and replaced with RPMI-1640 medium for differentiation with added 100 ng/mL NGF. For protein analysis, CHO-AA8-Lucl cells ($7.5 \times \sim 10^5$/well, Clontech) were transfected in the same way. After 24 h, cells were subjected to western blot analysis or immunocytochemical analysis.

Western blot analysis

Transfected CHO-AA8-Lucl cells were washed with PBS contained protease inhibitor and after collecting lysates in solution containing 20 mM Tris-base, 0.1% SDS, 1% sodium deoxycholate, 1% Triton X-100 and 0.001 g/5 mL protease inhibitor and then centrifuged at 15 000 r.p.m. for 30 min at 4°C. After collecting supernatant, protein concentrations of lysates were determined using Bio-Rad protein assay kits (Bio-Rad, Hercules, CA, USA). Lysates were boiled for 10 min, resolved by 10–20% gradient SDS-PAGE, and transferred to polyvinylidene difluoride membranes (Bio-Rad) with a semidry electroblotter (Bio-Rad). The membrane was blocked by incubation in 1% BSA/TBST for 1 h at room temperature. Anti-PGP9.5 (UCH L1) antibody (1 : 100, Medac) was used as a primary antibody in Western blotting. Anti-rabbit IgG conjugated with

horseradish peroxidase (1: 2000) (Dako, Carpinteria, CA, USA) was used as secondary antibody. Immunoreactive bands were detected using the supersignal substrate system (Pierce, Rockford, IL, USA) according to manufacturer's instructions.

Immunocytochemical analysis

After transfection, cells were fixed with 4% paraformaldehyde. Immunocytochemistry on CHO-AA8-Lucl cells and PC12 Tet-Off cells was performed as previously described (Osaka *et al.* 2003) using antibodies to ubiquitin that is predominantly reactive to free ubiuitin in immuno-histochemistry (1 : 100, Sigma; polyclonal) and UCH L1 (1 : 100, Medac; monoclonal). For immunofluorescence studies, antirabbit IgG conjugated with Cy3 antibodies (1 : 200, Jackson Immuno Research) and antirabbit IgG conjugated with Alexa Fluor 568 antibodies (1 : 1000, Molecular Probes) were used as secondary antibodies. Also, in PC12 Tet-Off cells, 300 μM DAPI was applied to stain transfected and untransfected cell nuclei for 5 min, and then the cells were washed with PBS for 5 min at least five times. Twenty confocal images with 0.5 μm width were obtained and reconstructed using the confocal laser microscope system (Radiance2100, Bio-Rad). To stain mono-ubiquitin, the same laser strength was used in mock, wild-type and C90S UCH L1-transfeacted cells under the confocal laser microscope system (LSM510, Carl Zeiss, Germany).

Electrophysiological measurements

The cell with fluorescence was chosen under the fluorescence microscope. Then, the patch pipette was applied to the cell to obtain a giga-ohm seal under the phase bright mode. Whole-cell recordings were made as reported previously (Noda *et al.* 1999, 2000), using an Axopatch-200B amplifier (Axon Instruments, Foster City, CA, USA), under voltage-clamp condition at the holding potential of −70 mV. Membrane currents were measured using a patch pipette containing (in mM): CsCl, 120; Mg_2ATP_3, 3; HEPES, 20; $CaCl_2$, 1; $MgCl_2$, 1; EGTA, 5. The pH of the solution was adjusted to 7.2 with 1 N CsOH. The pipette resistance was 5–9 MΩ. The external solution contained (mM): NaCl, 132; KCl, 5; $CaCl_2$, 2; $MgCl_2$, 1; glucose, 10; and HEPES, 10. The pH was adjusted to 7.4 with 1 N NaOH. External ATP or drugs were applied rapidly using the 'Y tube' technique (Min *et al.* 1996), which allows the complete exchange of the external solution surrounding a cell within 20 ms. Temperature monitored in the recording dishes was 33–34°C.

In the experiments using inhibitors except PD98059, ATP was applied twice to ensure reproducibility of the ATP-induced current in control experiments. The inhibitor solution was applied after first application of ATP for the period according to the references for each inhibitor until the end of second application of ATP. The current amplitude obtained at the second application of ATP with or without inhibitors normalized to the first ATP-induced current. All values were presented as means ± SEM. Statistical analysis was done using ANOVA. A value of $p < 0.05$ was considered to be the minimum level of significance. Curve fitting was performed using Hill Equation (Igor Pro 4.07; Wavemetrics, Lake Oswego, OR, USA).

SYBR Green-based Real-Time Quantitative RT–PCR

Total RNAs were prepared from 2×10^6 PC12 Tet-Off cells and a rat brain with RNeasy™. RNA purification kit (QIAGEN, Valencia, CA, USA) according to the manufacturer's protocol. First-strand cDNA synthesized from 1 μg total RNA with random hexamer primers was used as template for each reaction. SYBR Green-based Real-time Quantitative RT-PCR was performed as described (Wong *et al.* 2000; Aoki *et al.* 2002). Applied Biosystems 7700 Sequence Detection System was used for the signal detection and the PCR was performed in 1 × SYBR Green Master mix (Applied Biosystems, Foster City, CA, USA) and 50 nM of each primer. For standardization and quantification, rat β-actin or rat glyceraldehyde 3-phosphate dehydrogenase (GAPDH) was amplified simultaneously. Primer sequences were designed with Primer Express™ Software (Applied Biosystems). The following primer pairs were employed: 5′-TGCAGACCATCAGCAACCTG-3′ (upper, 17–36) and 5′-CTTGTGGATACCCCAGCTCC-3′ (lower, 103–84) for amplification of rat DARPP-32 (primer set A; GenBank accession No. AF281661): 5′-CACCTGCAGACCATCAGCAA-3′ (upper, 13–32) and 5′-CCTCTTGTGGATACCCCAGC-3′ (lower, 106–87) for amplification of rat DARPP-32 (primer set B; AF281661): 5′- ATCGCTGACAGGATGCAGAAG-3′ (upper, 925–945) and 5′-AGAGCCACCAATCCACACAGA-3′ (lower, 1032–1012) for amplification of rat β-actin: and 5′-ACCACAGTCCATGCCATCAC-3′ (upper, 586–605) and 5′- TCCACCACCCTGTTGCTGTA-3′ (lower, 1037–1018) for amplification of rat GAPDH. PCR conditions were: 95°C for 10 min, followed by 40 cycles at 95°C for 15 s and 60°C for 1 min. The threshold cycle of each gene was determined as the PCR cycle at which an increase in fluorescence was observed above the baseline signal in an amplification plot (Wada *et al.* 2000). The 'normalized expression level of target' (dCt) was calculated as the difference in threshold cycles for target and reference (β-actin or GAPDH). Subtraction of dCt for PC12 Tet-Off cells from dCt for the rat brain provided the ddCt value. The formula, 2^{-ddCt}, was used to calculate relative expression levels for PC12 Tet-Off cells compared to the rat brain. To reduce possible error, RT-PCR reaction was performed three times and averaged 2^{-ddCt} values were obtained. In addition, two gene-specific primer sets (set A and B, see above) for DARPP-32 gene and two independent RNA pools were examined to confirm DARPP-32 gene expression.

Drugs and reagents

RPMI-1640 medium, ATP-2Na, H-89, chelerythrine, roscovitine, PD98059, forskolin and 1,9-dideoxyforskolin were from SIGMA (St. Louis, MO, USA). NGF and Lipofectamine 2000 were from Gibco/BRL (Grand Island, NY, USA). KN-93 and okadaic acid was from CALBIOCHEM (San Diego, CA, USA).

Results

Transfection of UCH L1 in PC12 Tet-Off cells

Expression activity of plasmid constructs was first examined in CHO-AA8-Lucl cells that lack endogenous expression of UCH L1 (Fig. 1). Confocal microscopic examination revealed that UCH L1 immunoreactivity colocalizes with GFP fluorescence (Fig. 1a). Western blot analysis showed bands immunostained by anti-UCH L1 antibodies were

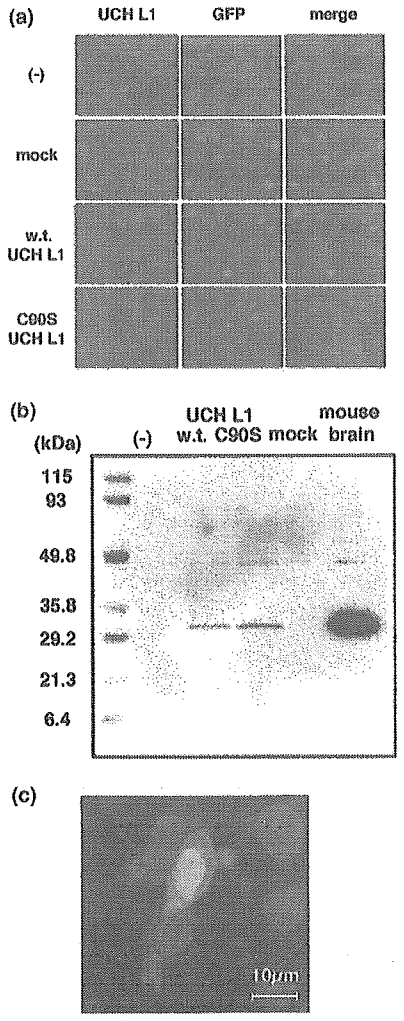

Fig. 1 Transfection efficacy of UCH L1 in CHO-AA8-LucI cells and PC12 Tet-Off cells. (a) Confocal image of CHO-AA8-LucI cells 24 h after transfection of pBI-EGFP-mock, wild type UCH L1 and C90S UCH L1 with Lipofectamine 2000 were double stained with UCH L1 (red). Cells with green fluorescence (GFP) are the transfected cells. (b) Western-blot analysis of CHO-AA8-LucI cells 24 h after transfection of pBI-EGFP-mock, -wild type UCH L1 and -C90S UCH L1 with Lipofectamine 2000. CHO-AA8-LucI cells were lysed with TBS buffer containing 0.1% Triton X. 10 μg of each protein was subjected to SDS-PAGE and immunoblotted with anti-PGP9.5 antibody. (c) Confocal image of overexpressed UCH L1 in PC12 Tet-Off cells were double stained with GFP (green) and DAPI (blue).

detected in cells transfected with pBI-EGFP-wild type UCH L1 or C90S UCH L1, but not mock plasmids (Fig. 1b). Figure 1(c) shows a PC12 Tet-Off representative cell with green fluorescence used for electrophysiological recording, although DAPI staining was not employed for the recording. The efficacy of the transfection was about 10% in PC12 Tet-Off cells.

Effects of overexpression of UCH L1 on ATP-induced currents

ATP-activated inward currents due to the activation of P2X receptors at the negative holding potential in PC12 cells were reported (Nakazawa *et al.* 1994). In our experiments, PC12 Tet-Off cells were voltage clamped at −70 mV and high concentration of ATP were used to see whether or not overexpression of UCH L1 affected maximum inward currents. In UCH L1-transfected PC12 Tet-Off cells, ATP-induced inward currents were significantly larger than those in mock-transfected cells. Unexpectedly the mutant (C90S) UCH L1, which lacks C-terminal hydrolase activity but retains ubiquitin binding affinity, had a similar effect to wild-type UCH L1 (Fig. 2a). The amplitude of peak inward currents in mock-, wild-type UCH L1- and C90S UCH L1-transfected PC12 Tet-Off cells were 15.0 ± 1.6 pA/pF ($n = 5$), 48.5 ± 6.0 pA/pF ($n = 6$) and 47.6 ± 4.1 pA/pF ($n = 6$), respectively (Fig. 2b).

The current-voltage relationships of ATP-induced inward currents were analyzed by applying voltage steps of 10 mV increments between −100 mV and + 50 mV with 50 ms duration and 50 ms interval from the holding potential of −70 mV before and during the application of ATP (Fig. 3a). The current traces before and after application of ATP in wild-type UCH L1-transfected PC12 Tet-Off cells were shown by applying voltage steps (Fig. 3b). Holding currents were negligibly misaligned even during the application of ATP. The current levels at the end of each pulse before and during ATP application were obtained in mock-, wild-type UCH L1- or C90S UCH L1-transfected PC12 Tet-Off cells.

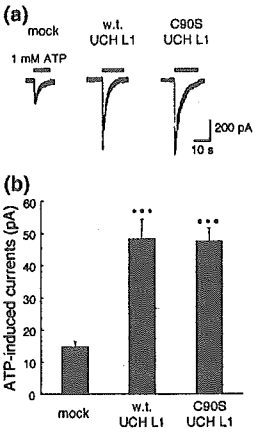

Fig. 2 Current amplitudes of ATP-induced currents in mock-, wild-type UCH L1- and C90S UCH L1-transfected PC12 Tet-Off cells. (a) Inward membrane currents induced by 1 mM ATP at the holding potential of −70 mV in mock-, wild-type (wt) and C90S UCH L1-transfected PC12 Tet-Off cells. (b) Amplitudes of peak inward currents induced by 1 mM ATP in mock-, wild-type and C90S UCH L1-transfected PC12 Tet-Off cells. The bars represent the mean ± SEM. ***: $p < 0.001$.

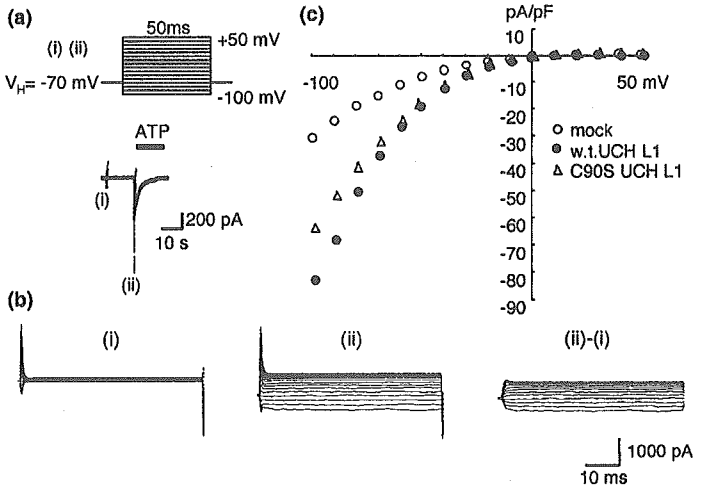

Fig. 3 Voltage-dependency of ATP-induced currents in mock-, wild-type UCH L1- and C90S UCH L1-transfected PC12 Tet-Off cells. A: The voltage protocol shown in the upper panel was applied before and during application of 1 mM ATP at the time indicated by (i) and (ii) in the lower panel. (b) Cumulated current traces obtained in wild type UCH L1-transfected cells before (i) and during (ii) application of ATP. The subtracted current traces [(i)-(ii)] show the ATP-induced currents. (c) The current–voltage relationships of ATP-induced currents. The amplitudes of subtracted currents [(ii)-(I)] in (b) at the end of 50 ms pulses were plotted against the pulse potentials in mock- (O), wild-type (●) and C90S UCH L1-transfected cells (△).

Then the amplitudes of ATP-induced currents at different voltages were obtained by subtracting the one before application of ATP from the one during application of ATP, and were plotted as in Fig. 3(c). In consideration of desensitization, the current-voltage relationships were obtained by applying voltage steps in opposite direction, i.e. from + 50 to − 100 mV, but there was almost no change (data not shown). The reversal potential was about 0 mV, suggesting that these currents were due to non-specific cationic channels.

ATP-induced inward currents were concentration dependent and the sensitivity of ATP was not significantly changed by overexpression of either wild- or C90S UCH L1. Each EC_{50} was 34 μM, 40 μM and 62 μM and each Hill coefficient (n_H) was 1.38, 1.48 and 1.34 in mock-, wild-type and C90S UCH L1-transfected cells, respectively (Fig. 4).

Effects of wild type and C90S UCH L1 on mono-ubiquitin expression

It was reported that absence of UCH L1 reduced the mono-ubiquitin level in mouse brain and UCH L1 overexpression increased the level of mono-ubiquitin by alteration of ubiquitin metabolism in cultured cells. Therefore, UCH L1-mediated increases in ubiquitin levels are a function of UCH L1 affinity for ubiquitin rather than hydrolase activity (Osaka *et al.* 2003). To clarify the effect of UCH L1 on ubiquitin levels in PC12 Tet-Off cells, ubiquitin was visualized using confocal immunofluorescence microscopy (Fig. 5). Wild-type UCH L1-transfected cells showed stronger immunoreactivity for ubiquitin compared with those in mock-transfected cells or non-transfected cells in the same field. Increased ubiquitin immunoreactivity was also evident in C90S UCH L1-transfected cells. These results were consistent with the previous report that ubiquitin were up-regulated by UCH L1 (Osaka *et al.* 2003).

Effects of Kinase inhibitors on ATP-induced currents in UCH L1-transfected cells

The mechanism by which ATP-induced currents were augmented in UCH L1-transfected cells was investigated. It was reported that in *Aplysia* UCH activated PKA as a result of the degradation of regulatory subunit of PKA, which contributed the long-term potentiation (Hegde *et al.* 1997). Therefore, the possibility of the involvement of the activated PKA was tested by using H-89, a PKA inhibitor. After obtaining a large ATP-induced currents in the UCH L1-transfected cells, 10 μM H-89 was applied for 10 min. The amplitude of ATP-induced currents in the presence of H-89 was 48.1 ± 3.51% (n = 8) compared to the first ATP-induced current in the same cell (control without H-89; 71.2 ± 5.6% (n = 7)) (Fig. 6a). Also, it was reported that the intracellular carboxyl terminus of P2X receptor contains several consensus phosphorylation sites for PKC as well as PKA, suggesting that the function of the P2X receptor could be regulated by protein phosphorylation (Chow and Wang 1998). Hence, the possibility of the involvement of the activated PKC was tested by using chelerythrine, a PKC inhibitor. Application of 5 μM chelerythrine for 10 min had no effect on the ATP-induced inward current in the UCH L1-transfected cell. The relative amplitude of second

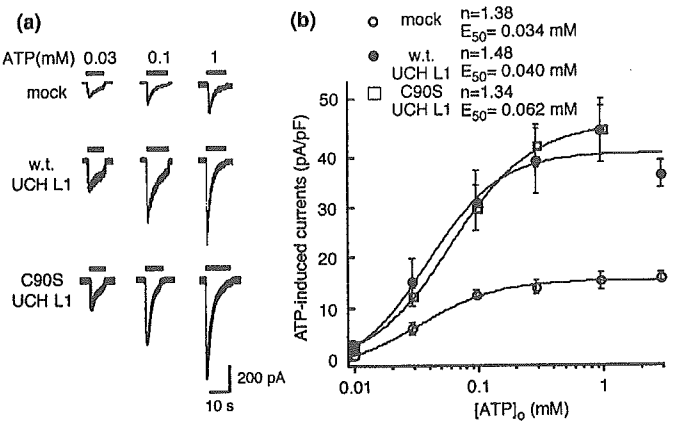

Fig. 4 Concentration-dependent curve of ATP-induced currents in mock-, wild-type and UCH L1-transfected PC12 Tet-Off cells. (a) Inward membrane currents induced by 0.03, 0.1 and 1 mM ATP at the holding potential of −70 mV in mock-, wild-type and C90S UCH L1-transfected PC12 Tet-Off cells. (b) The peak inward current induced by ATP at the holding potential of −70 mV was plotted against the ATP concentration between 0.01 and 3 mM in mock (○)-, wild-type (●) and C90S UCH L1 (□)-transfected PC12 Tet-Off cells. Each point represents the mean of five or six cells and the bar shows ± SEM. The curve shows the least squares fit, where n_H = Hill coefficient and EC_{50} = the half maximum concentration.

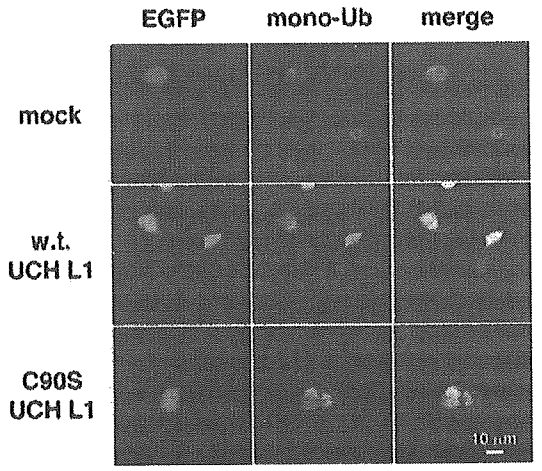

Fig. 5 Effects of wild-type and C90S UCH L1 on mono-ubiquitin expression. Confocal image of PC12 Tet-Off cells transfected pBI-EGFP-mock, wild-type (wt) UCH L1 and C90S UCH L1 with Lipofectamine 2000 were double stained with mono-ubiquitin (red) and GFP (green).

ATP-induced inward currents in the presence of chelerythrine was 71.9 ± 4.2% (n = 7) (control without chelerythrine; 71.2 ± 5.6% (n = 7)) (Fig. 6a). Furthermore, the possibility of the involvement of CaMKII was also tested by using KN-93, a CaMKII inhibitor. Application of 10 μM KN-93 for 20 min significantly reduced the ATP-induced inward current in the UCH L1-transfected cell (69.9 ± 6.7% (n = 5); control, 90.2 ± 3.5% (n = 5)) (Fig. 6b).

In UCH L1-transfected PC12 Tet-Off cells, increased ATP-induced currents were not completely reversed by H-89 or KN-93, suggesting that both PKA and CaKII contributed independently. Hence, the combination of PKA and CaMKII was tested to see whether coapplication of H-89 and KN-93 inhibited the effect of UCH L1 additively. Coapplication of 10 μM KN-93 and 10 μM H-89 attenuated ATP-induced currents more strongly than that with single kinase inhibitor. The relative amplitude of ATP-induced inward currents was 45.8 ± 2.7% (n = 7) (control without inhibitors; 90.2 ± 3.5% (n = 5)) (Fig. 6b).

In PC12 cells and hippocampal neurons, it was reported that activation of PKA caused activation of extracellular signal-regulated kinase (ERK), subsequent phosphorylation of Ca^{2+}-stimulated cAMP response element binding protein (CREB) and stimulated transcription. Such signal transduction was predicted to contribute to long-term potentiation (Impey *et al.* 1998). Likewise, the augmentation of ATP response in UCH L1-transfected cell might be due to the stimulation of transcription that increased the number of P2X receptors. To test this possibility, we examined whether mitogen-activated protein kinase (MAPK) including ERK was activated following the activation of PKA in PC12 Tet-Off cells. The result was that even after application of cells with 5 μM PD98059, one of the MAPK kinase inhibitors, for 4 days, ATP-induced currents in UCH L1-transfected cells were not affected. The amplitude of ATP-induced inward currents after the application of PD98059 was 53.3 ± 3.5 pA/pF (n = 2) (control without PD98059; 50.8 ± 5.2 pA/pF (n = 8)) (Fig. 6c).

Expression of DARPP-32 in PC12 Tet-Off cells

In rat striatum, positive feedback mechanism of dopamine signaling via PKA was reported. Activation of PKA causes phosphorylation at threonine 34 (Thr-34) of dopamine and cAMP-regulated phosphoprotein with molecular weight of

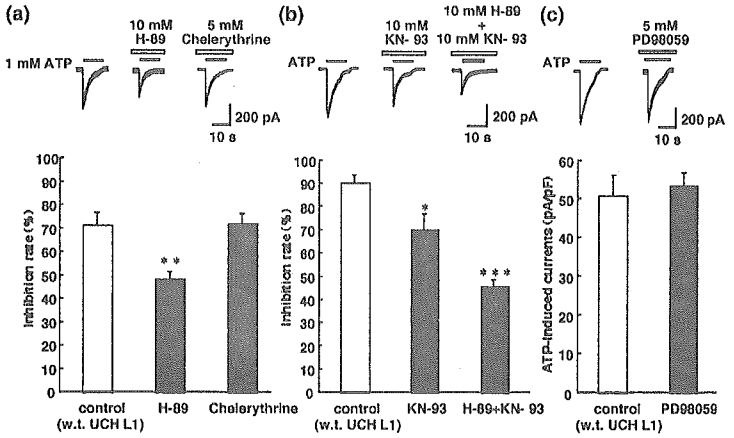

Fig. 6 Inhibition of ATP-induced currents by kinase inhibitors in wild type UCH L1-transfected PC12 Tet-Off cells. (a) ATP-induced currents were attenuated by pre-application of 10 μM H-89, a PKA inhibitor, but not by 5 μM chelerythrine, a PKC inhibitor, for 10 min. (b) ATP-induced currents were attenuated by pre-application of 10 μM KN-93, a CaMKII inhibitor, for 20 min. ATP-induced currents were further attenuated by copreapplication of 10 μM KN-93 and 10 μM H-89. C: ATP-induced currents were not affected by application of 5 μM PD98059, a MAPKK inhibitor, for four days. $^{*}p < 0.05$, $^{**}p < 0.01$, $^{***}p < 0.001$.

about 32 000 (DARPP-32), which reduces PP1 activity and consequently inhibits dephosphorylation of various substrates in the cell. On the other hand, activation of PKA stimulates PP2A activity and suppresses the phosphorylation at Thr-75 of DARPP-32. Since phosphorylation of DARPP-32 at Thr-75 has negative feedback regulation on PKA activity, dephosphorylation at Thr-75 reduces the inhibition of PKA activity (Nishi *et al.* 2000). To examine whether the similar mechanism exists in PC12 Tet-Off cells, we analyzed the expression of DARPP-32 first. With RT-PCR method using two kinds of primer sets specific to DARPP-32 (primer set A and B), the relative expression levels of DARPP-32 in rat whole brain and PC12 Tet-Off cells under non-differentiated and differentiated conditions were compared. As shown in Fig. 7(a), DARPP-32 was expressed in PC12 Tet-Off cells and the expression level tended to increase after differentiation of the cells with NGF. The possibility of the involvement of DARPP-32 and its phosphorylation was further tested using okadaic acid, a PP1 and PP2A inhibitor. The relative amplitudes of ATP-induced inward currents after the application of 100 nM okadaic acid for 20 min was significantly inhibited to 49.9 ± 11.1% ($n = 5$) (control without okadaic acid; 90.2 ± 3.5% ($n = 5$)), presumably due to the inhibition of PP2A and subsequent dephosphorylation of Thr-75, leading the release of negative feedback on PKA (Fig. 7b). Since phosphorylation of Thr-75 was also

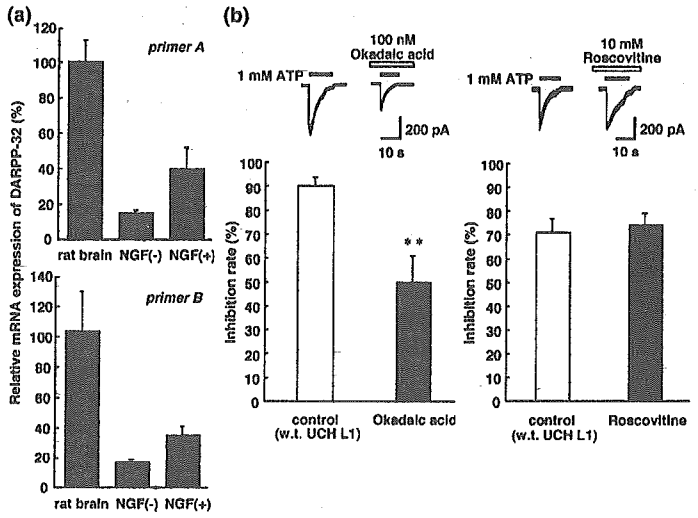

Fig. 7 Quantitative RT–PCR of DARPP-32 and effects of okadaic acid and roscovitine on ATP-induced currents in wild-type UCH L1-transfected PC12 Tet-Off cells. (a) The expression level of DARPP-32 mRNA was normalized to that of rat brain β-actin mRNA. Using two kinds of primer (a and b), PC12 Tet-Off cells were shown to express DARPP-32 whose level was increased by differentiation of the cells with NGF. B: ATP-induced currents were attenuated by preapplication of 100 nM okadaic acid, a PP1 and PP2 inhibitor, for 20 min. (c) ATP-induced currents were not affected by pre-application 10 μM roscovitine, a CDK5 inhibitor, for 10 min $^{**}p < 0.01$.

mediated by cycline-dependent kinase (CDK), the effect of a CDK inhibitor was tested to see if ATP-induced currents were more enhanced. However, application of 10 μM roscovitine for 10 min did not have significant effect (74.4 ± 5.1% (n = 4); control; 71.2 ± 5.6% (n = 7)) (Fig. 7c).

ATP-induced currents in mock-transfected cells

We concluded that the increase of ATP-induced inward currents in UCH L1-transfected cells was partly attributed to the activation of PKA. Hence, we tested whether ATP-induced currents in the cells not transfected with UCH L1 were increased by the application of forskolin, an adenylate cyclase activator that increases intracellular level of cAMP (Conn *et al.* 1989). The ATP-induced currents in mock-transfected cells were significantly increased after the application of 10 μM forskolin for 10 min (109.2 ± 2.2% (n = 5); control without forskolin; 87.4 ± 3.8% (n = 5)) (Fig. 8a). It was confirmed that application of inactive analogue of forskolin, 10 μM 1,9-dideoxyforskolin, did not have such effect (79.2 ± 2.2% (n = 5); control; 87.4 ± 3.8% (n = 5)) (Fig. 8a). Next, the effects of kinase inhibitors on ATP-induced currents were tested in mock-transfected cells. In mock-transfected cells, application of 10 μM H-89 for 10 min or 10 μM roscovitine for 10 min had no effect on the ATP-induced inward current (H-89, 84.3 ± 3.0% (n = 4); roscovitine, 93.4 ± 5.0% (n = 4); control; 87.4 ± 3.8% (n = 5)) (Fig. 8a). On the other hand, ATP-induced inward currents were significantly increased after application of 100 nM okadaic acid for 20 min (62.5 ± 6.7% (n = 5)). However, application of 10 μM KN-93 had no effect (111.3 ± 7.1% (n = 3); control; 79.0 ± 3.8% (n = 5)) (Fig. 8b).

ATP-induced currents in C90S UCH L1-transfected cells

Since ATP-induced currents in and C90S UCH L1-transfected PC12 Tet-Off cells were significantly potentiated as well, the same pharmacological analyses were done to see whether or not the mechanism was the same as in wild-type UCH L1-transfected cells. Application of 10 μM H-89 for 10 min significantly reduced ATP-induced currents in C90S UCH L1-transfected cells (61.9 ± 2.0% (n = 8); control without H-89, 78.4 ± 3.3% (n = 4)) (Fig. 9a). Also, applications of 10 μM KN-93 or 100 nM okadaic acid for 20 min significantly reduced ATP-induced inward currents in C90S UCH L1-transfected cells (KN-93, 58.0 ± 3.7% (n = 5); okadaic acid, 65.1 ± 4.9% (n = 6); control; 88.0 ± 3.4% (n = 5)) (Fig. 9b). Furthermore, ATP-induced currents were more attenuated by copreapplication of 10 μM KN-93 and 10 μM H-89 (44.2 ± 3.7% (n = 6); control; 88.0 ± 3.4% (n = 5)) (Fig. 9b).

Discussion

To analyze the functional role of UCH L1 in the central nervous system (CNS), it is important to know whether UCH L1 has any effects on ion channels and receptors that are the basic elements of neurotransmission. There are many ways to analyze them, but one of the most simple but efficient ways to start is to analyze the effects of exogenous UCH L1 in neuronal cultured cell line. To confirm that cells express the transfected protein, we used CHO-AA8-Lucl cells because of the higher transfection efficacy and not having endogenous UCH L1 (Fig. 1). For functional analyses of UCH L1 in nervous system, we used PC12 Tet-Off cells. The engineered PC12 cells are constructed to have higher transfection efficiency than wild-type PC12 cells which are one of the popular neuronal cell line (unpublished data). Among neurotransmitter receptors in PC12 cells, we analyzed ATP-activated receptors that are widely distributed in the brain and involved in various biological activities including neurosecretion. In PC12 cells, $P2X_2$ and $P2X_4$ receptors (Hur *et al.* 2001) with lower level of $P2X_6$ (unpublished data) are expressed and ATP-induced inward currents were well characterized (Nakazawa *et al.* 1994). We recorded

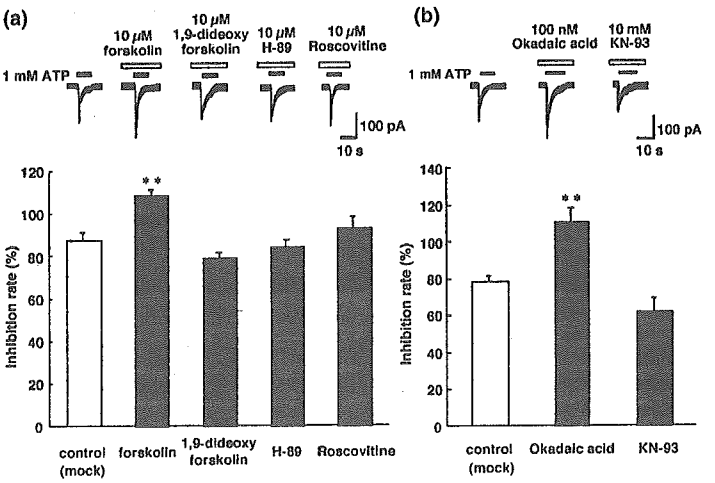

Fig. 8 ATP-induced currents in mock-transfected PC12 Tet-Off cells. (a) ATP-induced currents were augmented by preapplication of 10 μM forskolin for 10 min, but were not affected by 10 μM H-89 and 10 μM roscovitine. (b) ATP-induced currents were augmented by 100 nM okadaic acid, but were not affected by 10 μM KN-93. $^{**}p < 0.01$.

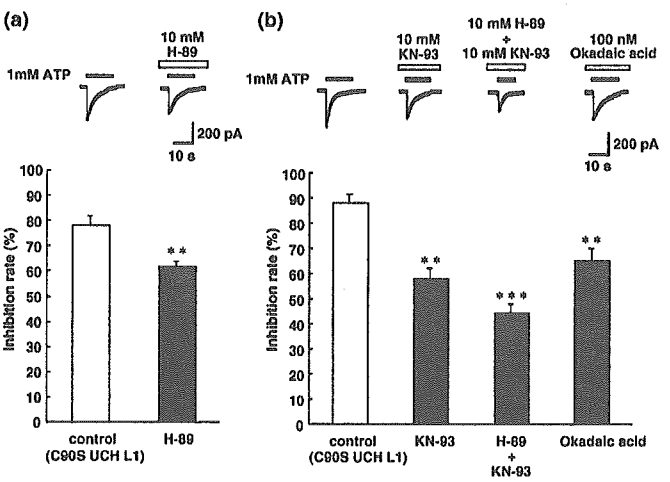

Fig. 9 ATP-induced currents in C90S UCH L1-transfected PC12 Tet-Off cells were also dependent on PKA and CaMKII. (a) ATP-induced currents were attenuated by pre-application of 10 μM H-89 for 10 min. (b) ATP-induced currents were attenuated by preapplication of 10 μM KN-93 and 100 nM okadaic acid for 20 min. ATP-induced currents were further attenuated by copreapplication of 10 μM H-89 and 10 μM KN-93. $^{**}p < 0.01$, $^{***}p < 0.001$.

ATP-induced inward currents due to the activation of P2X receptor channels at the holding potential of −70 mV under the conventional whole-cell patch clamp configuration. To analyze the effects of overexpression of UCH L1 and for pharmacological characterization, high concentration of ATP (1 mM) was used to see the effects on the maximum response to ATP. As to the possibility to analyze other receptor channels expressed in PC12 cells, nicotinic acetylcholine receptor (nAChR) was likely to be analyzed. However, no currents were recorded using ACh or nicotine (not shown), probably because nAChR required longer time to be expressed after differentiation (Fukukawa *et al.* 1992).

The amplitude of ATP-induced inward currents was significantly greater in both wild-type and mutant (C90S) UCH L1-transfected PC12 Tet-Off cells (Fig. 2a). We found that the potentiation of ATP-induced currents was due to the activation of PKA and CaMKII (Fig. 6). Though activation of PKA by homologous UCH was reported in *Aplysia* (Hegde *et al.* 1997), the mechanism of PKA activation in PC12 cells would be different from the one in *Aplysia*. In *Aplysia*, UCH enhances the degradation of the regulatory subunit of PKA and consequently activate PKA. However, in our study, the mutant (C90S) UCH L1, which lacks hydrolase activity, also potentiated ATP-induced currents, which was also attenuated by H-89 and KN-93 (Figs 2 and 9). Therefore, function of UCH L1 other than hydrolase activity should play a fundamental role. Based on the previous reports that UCH L1 has multifunction, one of the plausible reason would be the ability to increase free ubiquitin by both wild-type and C90S mutant UCH L1. It was reported that C90S UCH L1 lacks hydrolase activity, but retains ubiquitin binding affinity and increases free ubiquitin level in SH-SY5Y cells (Osaka *et al.* 2003). Actually, immunostaining of mono-ubiquitin was stronger in the cytoplasm of wild-type and C90S UCH L1-transfected PC12 Tet-Off cells (Fig. 5). The mechanism how increased level of mono-ubiquitin activated PKA and CaMKII were not yet known and should be investigated further.

The mechanism how activated PKA and CaMKII potentiate ATP-induced currents also remains to be investigated. One possible mechanism would be phosphorylation of P2X receptors by these protein kinases, though it was reported that activation of PKA reduced the magnitude of the ATP-activated current in $P2X_2$-transfected HEK293 cells (Chow and Wang 1998). The potentiation of ATP-induced currents by PKA in our study might be similar to the one observed for Ca^{2+} channels (Kamp and Hell 2000). Likewise, in mock-transfected cells, the amplitude of ATP-induced currents was significantly increased by forskolin, an adenylate cyclase activator that increases intracellular levels of cAMP and activates PKA (Fig. 8). Therefore, it was suggested that at least an activation of PKA contributed to the potentiation of ATP-induced currents. As for the involvement of CaMKII, it has been recently reported that CaMKII potentiates ATP responses by promoting trafficking of P2X receptors (Xu and Huang 2004), suggesting that phosphorylation of P2X receptors were not the sole mechanism of the potentiation of ATP-induced currents. Furthermore, since increased ATP-induced currents were not completely reduced by H-89, KN-93 nor coapplication of H-89 and KN-93 in wild-type or C90S UCH L1-transfected cells (Figs 6 and 9), it was also suggested that activation of PKA and CaMKII was not the sole mechanism of the potentiation of ATP-induced currents but there may be other components, too.

Another possible mechanism how PKA potentiates ATP-induced currents would be an increase in number of P2X receptors. In *Aplysia*, homologous UCH activates PKA and consequently activates MAPK and subsequent transcription (Hegde *et al.* 1997). Such signal transduction is predicted to contribute to a long-term potentiation (Impey *et al.* 1998). If the similar signaling exists in mammalian cells, the number of P2X receptors could increase during the differentiation

after transfection of UCH L1 or C90S UCH L1. However, it was unlikely because even after incubation with MAPK inhibitor during differentiation, the augmented ATP-induced currents were still observed in wild-type (Fig. 6c) or C90S UCH L1-transfected cells (not shown).

There may be indirect effects of phosphorylation by PKA on P2X receptors. In rat striatum, it has been suggested that there are positive and negative feedback system of DARPP-32 via activation of PKA and CDK5, respectively (Nishi *et al.* 2000). To test whether the similar mechanism exists in PC12 Tet-Off cells, we first analyzed the expression of DARPP-32 with RT-PCR. DARPP-32 was expressed in PC12 Tet-Off cells and we found that the expression level of DARPP-32 was increased after differentiation of the cells with NGF (Fig. 7). Thus, the possibility of the involvement of DARPP-32 in the P2X receptor activation was tested with using okadaic acid, a PP1 and PP2A inhibitor, and roscovitine, a CDK5 inhibitor. Roscovitine had no effects on the ATP-induced currents in mock- and UCH L1-transfected PC12 Tet-Off cells, suggesting that CDK5 did not play an important role in the regulation of P2X receptor via DARPP-32 in PC12 Tet-Off cells. On the other hand, the ATP-induced inward currents were attenuated by okadaic acid in wild-type or C90S UCH L1-transfected PC12 Tet-Off cells (Figs 7b and 9b), but increased in mock-transfected PC12 Tet-Off cells (Fig. 8b). Based on these results, we assume the followings; (1) In wild-type and C90S UCH L1-transfected cells, activation of PKA by wild-type or C90S UCH L1 stimulates PP2A activity and dephosphorylate DARPP-32 at Thr-75. Since phosphorylation of DARPP-32 at Thr-75 inhibits PKA activity, inhibition of PP2A by okadaic acid accelerates phosphorylation at Thr-75, which in turn has a negative feedback effect on PKA activity and their substrates. On the other hand, activation of PKA by wild-type or C90S UCH L1 causes phosphorylation at Thr-34 of DARPP-32, which in turn reduces PP1 activity. If PP1 activity is already low enough, okadaic acid does not have significant effect on dephosphorylation of P2X receptors and presumably other proteins by PP1 (Fig. 10, *right*). (2) In mock-transfected PC12 Tet-Off cells, PKA activity is supposed to be low, because H-89 did not have significant effect and forskolin augmented the ATP-induced currents (Fig. 8a). Under this condition, PP1 activity might be prominent, which dephosphorylates various substrates including P2X receptors. Without activation of PKA, less phosphorylation at Thr-34 and less activation of PP2A, which in turn cause more phosphorylation at Thr-75 (Fig. 10, *left*). Therefore inhibition of mainly PP1 by okadaic acid could prevent the dephosphorylation of P2X receptor, increasing ATP-induced currents. (3) In both UCH L1- and mock-transfected PC12 Tet-Off cells, phosphorylation of DARPP-32 at Thr-75 by CDK5 might be negligible and CDK5 signaling did not have significant effect, unlike in neostriatal neurons (Nishi *et al.* 2000; Bibb *et al.* 2001).

As a conclusion, our present observation indicates that UCH L1 potentiates ATP responses due to activation of P2X receptors by up-regulation of ubiquitin level, activation of PKA and CaMKII, and regulation of DARPP-32. As UCH L1 has multifunction and is known to be transported over long distances via slow axonal transport to synapses (Bizzi *et al.* 1991), UCH L1 is supposed to have various effects on neuronal function. Our finding shows the first evidence that there is a relationship between UCH L1 and neurotransmitter receptor, suggesting that UCH L1 may play an important role in synaptic activity. The question whether UCH L1 can affect other neurotransmitter receptors such as GABA and glutamate receptors should be investigated further. On the contrary, ubiquitin reduction and the consequent inadequate ubiquitination of proteins may trigger accumulation of proteins that should undergo ubiquitin-dependent degradation (Wang *et al.* 2004). The question whether lack of UCH L1 interfere the functional role of neurotransmitter receptors should be

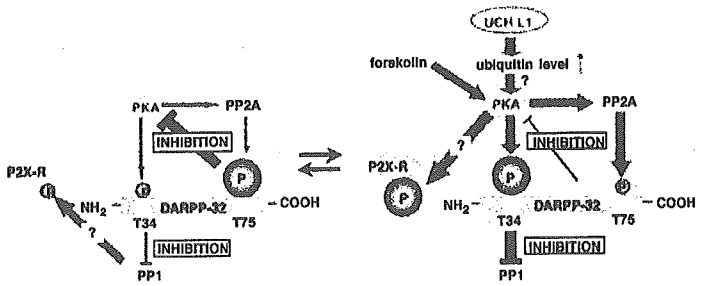

Fig. 10 Predicted PKA signaling via DARPP-32 in mock- and wild-type or C90S UCH L1 -transfected PC12 Tet-Off cells. Left: In mock-transfected cells, corresponding to basal condition, phosphorylation of DARPP-32 at Thr-75 has negative feedback effect on PKA, Down-regulation of PKA also results in less phosphorylation of DARPP-32 at Thr-34 and therefore less inhibition of PP1. Down-regulated PKA and PP1 are supposed to reduce the phosphorylation of P2X receptors. Right: In wild-type or C90S UCH L1-transfected cells, PKA is reported to activate PP2A, which dephosphorylate DARPP-32 at Thr-75, subsequently removing the negative feedback on PKA. Activation of PKA also results in the increased phosphorylation of DARPP-32 at Thr-34, which in turn inhibits PP1. Activation of PKA and inhibition of PP1 are supposed to increase the phosphorylation of P2X receptors.

investigated next. These studies may help to understand how dysfunction of UCH L1 causes neurodegeneration.

Acknowledgements

We thank Ms. Yuki Kosai for technical assistance in gaining confocal images. This work was supported by Grants-in Aid for Scientific Research of Japan Society for Promotion of Science, Grants-in Aid for Scientific Research in Priority Area Research of the Ministry of Education, Culture, Sports, Science and Technology, Japan, Kyushu University Foundation, Grants-in-Aid for Scientific Research of the Ministry of Health, Labour and Welfare, Japan and a grant from Pharmaceuticals and Medical Devices Agency, Japan.

References

Aoki K., Sun Y. J., Aoki S., Wada K. and Wada E. (2002) Cloning, expression, and mapping of a gene that is upregulated in adipose tissue of mice deficient in bombesin receptor subtype-3. *Biochem. Biophys. Res. Commun.* **290**, 1282–1288.

Bibb J. A., Chen J., Taylor J. R., Svenningsson P., Nishi A., Snyder G. L., Yan Z., Sagawa Z. K., Ouimet C. C., Nairn A. C., Nestler E. J. and Greengard P. (2001) Effects of chronic exposure to cocaine are regulated by the neuronal protein Cdk5. *Nature* **410**, 376–380.

Bizzi A., Schaetzle B., Patton A., Gambetti P. and Autilio-Gambetti L. (1991) Axonal transport of two major components of the ubiquitin system: free ubiquitin and ubiquitin carboxyl-terminal hydrolase PGP 9.5. *Brain Res.* **548**, 292–299.

Chow Y. W. and Wang H. L. (1998) Functional modulation of P2X2 receptors by cyclic AMP-dependent protein kinase. *J. Neurochem.* **70**, 2606–2612.

Cieehanover A., Orian A. and SchwartZ. A. L. (2000) The ubiquitin-mediated proteolytic pathway: Mode of action and clinical implications. *J. Cell Biochem.* **77**, 40–51.

Conn P. J., Strong J. A., Azhderian E. M., Nairn A. C., Greengard P. and Kaczmarek L. K. (1989) Protein kinase inhibitors selectively block phorbol ester- or forskolin-induced changes in excitability of Aplysia neurons. *J. Neurosci.* **9**, 473–479.

Coux O., Tanaka K. and Goldberg A. L. (1996) Structure and function of the 20S and 26S proteasomes. *Annu. Rev. Biochem.* **65**, 801–847.

Fukukawa K., Akaike M., Onodera H. and Kogure K. (1992) Expression of 5-HT3 receptor in PC12 cells treated with NGF and 8-Br.-cAMP. *J. Neurophysiol.* **67**, 812–819.

Harada T., Harada C., Wang Y. L., Osaka H., Amanai K., Tanaka K., Takizawa S., Setsuie R., Sakurai M., Sato Y., Noda M. and Wada K. (2004) Role of ubiquitin carboxy terminal hydrolase-l1 in neural cell apoptosis induced by ischemic retinal injury in vivo. *Am. J. Pathol.* **164**, 59–64.

Hegde A. N., Inokuchi K., Pei W., Casadio A., Ghirardi M., Chain D. G., Martin K. C., Kandel E. R. and SchwartZ. J. H. (1997) Ubiquitin C-terminal hydrolase is an immediate-early gene essential for long-term facilitation in Aplysia. *Cell* **89**, 115–126.

Huang Y., Baker R. T. and Fischer-Vize J. A. (1995) Control of cell fate by a deubiquitinating enzyme encoded by fat facets gene. *Science* **270**, 1828–1831.

Hur E. M., Park T. J. and Kim K. T. (2001) Coupling of l-type voltage-sensitive calcium channels to P2X (2) purinoceptors in PC-12 cells. *Am. J. Physiol. Cell Physiol.* **280**, C1121–C1129.

Ikeuchi Y., Nishizaki T., Mori M. and Okada Y. (1996) Regulation of the potassium current and cytosolic Ca^{2+} release induced by 2-methylthio ATP in hippocampal neurons. *Biochem. Biophys. Res. Commun.* **218**, 428–433.

Impey S., Obrietan K., Wong S. T., Poser S., Yano S., Wayman G., Deloulme J. C., Chan G. and Storm D. R. (1998) Cross talk between ERK and PKA is required for Ca^{2+} stimulation of CREB-dependent transcription and ERK nuclear translocation. *Neuron* **21**, 869–883.

Kamp T. J. and Hell J. W. (2000) Regulation of cardiac l-type calcium channels by protein kinase A and protein kinase C. *Circ Res.* **87**, 1095–1102.

King R. W., Deshaies R. J., Peters J.-M. and Kirschner M. W. (1996) How proteolysis drives the cell cycle. *Science* **274**, 1652–1659.

Kwon J., Wang Y. L., Setsuie R., Sekiguchi S., Sakurai M., Sato Y., Lee W. W., Ishii Y., Kyuwa S., Noda M., Wada K. and Yoshikawa Y. (2004a) Developmental regulation of ubiquitin C-terminal hydrolase isozyme expression during spermatogenesis in mice. *Biol. Reprod.* **71**, 515–521.

Kwon J., Wang Y. L., Setsuie R., Sekiguchi S., Sato Y., Sakurai M., Noda M., Aoki S., Yoshikawa Y. and Wada K. (2004b) Two closely related ubiquitin C-terminal hydrolase isozymes function as reciprocal modulators of germ cell apoptosis in cryptorchid testes. *Am. J. Pathol.* **165**, 1367–1374.

Leroy E., Boyer R., Auburger G., Leube B., Ulm G., Mezey E., Harta G., Brownstein M. J., Jonnalagada S., Chernova T., Dehejia A., Lavedan C., Gasser T., Steinbach P. J., Wilkinson K. D. and Polymeropoulos M. H. (1998) The ubiquitin pathway in Parkinson's disease. *Nature* **395**, 451–452.

Liu Y., Fallon L., Lashuel H. A., Liu Z. and Lansbury P. T. Jr (2002) The UCH-L1 gene encodes two opposing enzymatic activities that affect alpha-synuclein degradation and Parkinson's disease susceptibility. *Cell* **111**, 209–218.

Min B. I., Kim C. J., Rhee J. S. and Akaike N. (1996) Modulation of glycin-induced chloride current in acutely dissociated rat periaqueductal gray neurons by 1-opioid agonist DAGO. *Brain Res.* **734**, 72–78.

Muralidhar M. G. and Thomas J. B. (1993) The Drosophila bendless gene encodes a neural protein related to ubiquitin-conjugating enzymes. *Neuron* **11**, 253–266.

Nakazawa K., Inoue K., Koizumi S. and Inoue K. (1994) Facilitation by 5-hydroxytryptamine of ATP-activated current in rat pheochromocytoma cells. *Pflugers Arch.* **427**, 492–499.

Nishi A., Bibb J. A., Snyder G. L., Higashi H., Nairn A. C. and Greengard P. (2000) Amplification of dopaminergic signaling by a positive feedback loop. Proceedings *Natl. Acad. Sci. USA* **97**, 12 840–12 845.

Noda M., Nakanishi H. and Akaike N. (1999) Glutamate release from microglia via glutamate transporter is enhanced by amyloid-beta peptide. *Neuroscience.* **92**, 1465–1474.

Noda M., Nakanishi H., Nabekura J. and Akaike N. (2000) AMPA-KA subtypes of glutamate receptor in rat cerebral microglia. *J. Neurosci.* **20**, 251–258.

Oh C. E., McMahon R., Benzer S. and Tanouye M. A. (1994) bendless, a Drosophila gene affecting neuronal connectivity, encodes a ubiquitin-conjugating enzyme homolog. *J. Neurosci.* **14**, 3166–3179.

Osaka H., Wang Y. L., Takada K., Takizawa S., Setsuie R., Li H., Sato Y., Nishikawa K., Sun Y. J., Sakurai M., Harada T., Hara Y., Kimura I., Chiba S., Namikawa K., Kiyama H., Noda M., Aoki S. and Wada K. (2003) Ubiquitin carboxy-terminal hydrolase L1 binds to and stabilizes monoubiquitin in neuron. *Hum. Mol. Genet.* **12**, 1945–1958.

Rock K. L., Gram C., Rothstein L., Clark K., Stein R., Dick L., Hwang D. and Goldberg A. L. (1994) Inhibitors of the proteasome block the degradation of most cell proteins and the generation of peptides present on MHC class I molecules. *Cell* **78**, 761–771.

Saigoh K., Wang Y. L., Suh J. G., Yamanishi T., Sakai Y., Kiyosawa H., Harada T., Ichihara N., Wakana S., Kikuchi T. and Wada K. (1999)

Intragenic deletion in the gene encoding ubiquitin carboxy-terminal hydrolase in gad mice. *Nat. Genet.* **23**, 47–51.

Sela D., Ram E. and Atlas D. (1991) ATP receptor. A putative receptor-operated channel in PC-12 cells. *J. Biol. Chem.* **266**, 17 990–17 994.

Verma I. M., Stevenson J. K., SchwartZ. E. M., Van Antwerp D. and Miyamoto S. (1995) Rel/NF-κB/I-κB family: intimate tales of association and dissociation. *Genes Dev.* **9**, 2723–2735.

Wada R., Tifft C. J. and Proia R. L. (2000) Microglial activation precedes acute neurodegeneration in Sandhoff disease and is suppressed by bone marrow transplantation. *Proc. Natl. Acad. Sci. USA* **97**, 10 954–10 959.

Wang Y. L., Takeda A., Osaka H., Hara Y., Furuta A., Setsuie R., Sun Y. J., Kwon J., Sato Y., Sakurai M., Noda M., Yoshikawa Y. and Wada K. (2004) Accumulation of beta- and gamma-synucleins in the ubiquitin carboxyl-terminal hydrolase L1-deficient gad mouse. *Brain Res.* **1019**, 1–9.

Wilkinson K. D. (1995) Roles of ubiquitinylation in proteolysis and cellular regulation. *Annu. Rev. Nutr.* **15**, 161–189.

Wilkinson K. D., Deshpande S. and Larsen C. N. (1992) Comparisons of neuronal (PGP 9.5) and non-neuronal ubiquitin C-terminal hydrolases. *Biochem. Soc. Trans.* **20**, 631–637.

Wilkinson K. D., Lee K. M., Deshpande S., Duerksen-Hughes P., Boss J. M. and Pohl J. (1989) The neuron-specific protein PGP 9.5 is a ubiquitin carboxyl-terminal hydrolase. *Science* **246**, 670–673.

Wong M. H., Saam J. R., Stappenbeck T. S., Rexer C. H. and Gordon J. I. (2000) Genetic mosaic analysis based on Cre recombinase and navigated laser capture microdissection. *Proc. Natl. Acad. Sci. USA* **97**, 12 601–12 606.

Xu G. Y. and Huang L. Y. (2004) Ca^{2+}/calmodulin-dependent protein kinase II potentiates ATP responses by promoting trafficking of P2X receptors. *Proc. Natl Acad. Sci. USA* **101**, 11 868–11 873.

Zhu Y., Carroll M., Papa F., Hochstrazin M. E. and D'Andrea A. D. (1996) DUB-1, a deubiquitinating enzyme with growth-suppressing activity. *Proc. Natl. Acad. Sci. USA* **93**, 3275–3279.

Available online at www.sciencedirect.com
SCIENCE DIRECT®
Biochemical and Biophysical Research Communications 319 (2004) 50–57
BBRC
www.elsevier.com/locate/ybbrc

RNAi induction and activation in mammalian muscle cells where *Dicer* and *eIF2C* translation initiation factors are barely expressed

Noriko Sago,[a,b,1] Kazuya Omi,[a,b,1] Yoshiko Tamura,[a] Hiroshi Kunugi,[a] Teruhiko Toyo-oka,[c] Katsushi Tokunaga,[b] and Hirohiko Hohjoh[a,*]

[a] *National Institute of Neuroscience, NCNP, 4-1-1 Ogawahigashi, Kodaira, Tokyo 187-8502, Japan*
[b] *Department of Human Genetics, Graduate School of Medicine, The University of Tokyo, 7-3-1 Hongo, Bunkyo-ku, Tokyo 113-0033, Japan*
[c] *Department of Pathophysiology and Internal Medicine, The University of Tokyo, 7-3-1 Hongo, Bunkyo-ku, Tokyo 113-0033, Japan*

Received 25 February 2004
Available online 10 May 2004

Abstract

Dicer plays an important role in the course of RNA interference (RNAi), i.e., it digests long double-stranded RNAs into 21–25 nucleotide small-interfering RNA (siRNA) duplexes functioning as sequence-specific RNAi mediators. In this study, we investigated the expression levels of *Dicer* and *eIF2C1~4*, which, like *Dicer*, appear to participate in mammalian RNAi, in various mouse tissues. Results indicate that the levels of *eIF2C1~4* as well as *Dicer* are lower in skeletal muscle and heart than in other tissues. To see if RNAi could occur under such a condition with low levels of expression of *Dicer* and *eIF2C1~4*, we examined RNAi activity in mouse skeletal muscle fibers. The results indicate that RNAi can be induced by synthetic siRNA duplexes in muscle fibers. We further examined RNAi activity during myogenic differentiation of mouse C2C12 cells. The data indicate that although the expression levels of *Dicer* and *eIF2C1~4* decrease during the differentiation, RNAi can be induced in the cells. Altogether, the data presented here suggest that muscle cells retain the ability to induce RNAi, although *Dicer* and *eIF2C1~4* appear to be barely expressed in them.

Keywords: RNA interference; Dicer; eIF2C translation initiation factors; Muscle; C2C12 cell

RNA interference (RNAi) is the process of a sequence-specific post-transcriptional gene silencing triggered by double-stranded RNAs (dsRNAs) homologous to the silenced genes. This intriguing gene silencing has been found in various species including flies, worms, protozoa, vertebrates, and higher plants (reviewed in [1–4]). DsRNAs introduced or generated in cells are digested by an RNase III enzyme, Dicer, into 21–25 nucleotide (nt) RNA duplexes [5–8] and the resultant duplexes, referred to as small-interfering RNA (siRNA) duplexes, function as essential sequence-specific RNAi mediators in the RNA-induced silencing complexes (RISCs) [5,7]. Thus, Dicer appears to play an important role in the process of RNAi induction.

In mammalian cells except for a part of undifferentiated cells [9–12], long dsRNAs (>30 bp) can trigger a rapid and non-specific RNA degradation involving the sequence-non-specific RNase, RNase L [13], and a rapid translation inhibition involving the interferon-inducible, dsRNA-activated protein kinase, PKR, instead of induction of RNAi [14]. In contrast, chemically synthesised siRNA duplexes can induce the sequence-specific RNAi activity in mammalian cells without triggering the rapid and non-specific RNA degradation and translation inhibition [15]. Together, it is likely that RNAi activity induced by the long dsRNAs could be masked by those rapid responses to the long dsRNAs in most of mammalian cells.

It may be of interest to examine the role of Dicer in differentiated mammalian cells possessing the rapid responses to long dsRNAs. Mammalian dicer has been identified and found to be a large multi-domain

* Corresponding author. Fax: +81-42-346-1744.
E-mail address: hohjohh@ncnp.go.jp (H. Hohjoh).
[1] These authors contributed equally to this work.

0006-291X/$ - see front matter © 2004 Elsevier Inc. All rights reserved.
doi:10.1016/j.bbrc.2004.04.151

polypeptide (~215 kDa) characterised by containing a putative DExH/DEAH RNA helicase/ATPase domain, a PAZ domain, two RNase domains, and a dsRNA-binding domain [16–20]. The expression of *Dicer* appears to be ubiquitous, but the level of its expression varies among tissues. Of the tissues examined previously, skeletal muscle appeared to express *Dicer* at a low level, i.e., the *Dicer* transcript appeared to be barely detectable at least using RT-PCR [16,17].

In this study, we investigated not only RNAi activity but also the expression levels of *Dicer* and *eIF2C1~4*, which, like *Dicer*, appear to participate in mammalian RNAi [21,22], in mouse skeletal muscle fibers, and muscle cells that differentiated from mouse C2C12 cells. The results indicate that RNAi can be induced by synthetic siRNA duplexes in those cells although the expression levels of *Dicer* and *eIF2C1~4* are lower than those in other tissues and undifferentiated C2C12 cells.

Materials and methods

Preparation and culture of muscle fibers isolated from extensor digitorum longus in mice. Isolation of muscle fibers from mice was carried out as described previously [23]. Briefly, extensor digitorum longus (EDL) was isolated from mice (ICR mouse strain), treated with 0.5% type 1 collagenase (Washington biochemical) in Dulbecco's modified Eagle's medium (DMEM) (Sigma), and incubated at 37 °C for 90 min. After incubation, the EDL was dissociated into single muscle fibers by gently pipetting, and dissociated single fibers were plated on matrigel-coated 24-well culture plates (approximately 100 fibers/well). The muscle fibers were cultured at 37 °C in DMEM supplemented with 10% horse serum (Invitrogen) in a 5% CO_2-humidified chamber. Two–three hours after starting culture, transfection was carried out.

Cell culture. C2C12 cells were grown at 37 °C in DMEM supplemented with 15% fetal calf serum (Sigma), 100 U/ml penicillin (Invitrogen), and 100 μg/ml streptomycin (Invitrogen) in a 5% CO_2-humidified chamber. For induction of myogenic differentiation, cells were cultured at 37 °C in DMEM supplemented with 5% horse serum (Invitrogen) in a 5% CO_2-humidified chamber [24]. The medium was changed everyday.

Synthetic oligonucleotides. RNA and DNA synthetic oligonucleotides were obtained from PROLIGO and SIGMAGENOSIS, respectively. The La2 siRNA duplex described previously was used in this study, and preparation of RNA duplexes was performed as described previously [25].

Transfection and luciferase assay. Reporter plasmids and siRNA duplexes were cotransfected into isolated single muscle fibers and undifferentiated and differentiated C2C12 cells using Lipofectamine 2000 (Invitrogen) according to the manufacturers' instructions. When undifferentiated C2C12 cells were used, the day before transfection, the cells were trypsinised, diluted with the fresh medium without

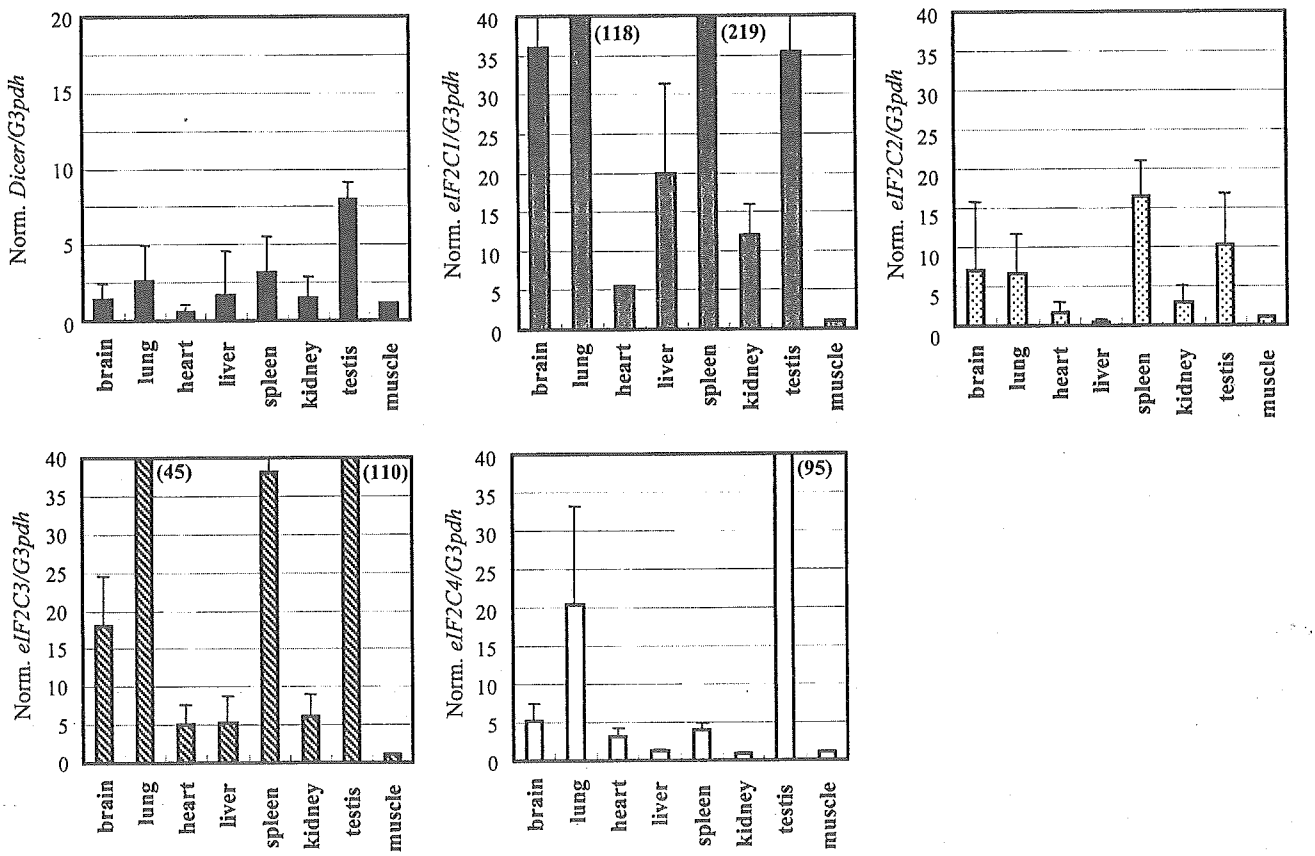

Fig. 1. Expression profiles of *Dicer* and *eIF2C1~4* in various mouse tissues. Total RNA was extracted from indicated tissues and subjected to cDNA synthesis with oligo(dT) primer and a reverse transcriptase. The expression levels of *Dicer* and *eIF2C1~4* were examined by means of a real-time PCR using the synthesised cDNAs as templates. The expression levels of the genes are normalised to that of the *G3pdh* gene examined as a control, and plotted when the expression level of either *Dicer* or *eIF2C1~4* in skeletal muscle is given as 1. Figures in parentheses indicate the averaged expression levels which are over the plotted areas. Data are averages of three independent experiments. Error bars represent standard deviations.

antibiotics, and seeded into 24-well culture plates (approximately 5×10^4 cells/well). Before the transfection, the culture medium was replaced with 0.5 ml OPTI-MEM I (Invitrogen), and to each well, 0.25 μg pGL3-control plasmid (Promega), 0.05 μg pRL-SV40 plasmid (Promega), and 0.2 μg siRNAs were applied. After 4-h incubation, 0.5 ml of the fresh culture medium without antibiotics was added, and further incubation at 37 °C was carried out. In the case of transfection into the isolated muscle fibers, the transfection mixture was directly applied into wells, and further incubation at 37 °C was carried out. When a short-hairpin expression plasmid, pRNA-U6.1/Neo/siRNA (GenScript), was used instead of synthetic siRNAs, 0.1 μg pGL3-control and 0.05 μg phRL-TK (Promega) together with various amounts of pRNA-U6.1/Neo/siRNA were introduced into C2C12 cells. The expression of luciferase was examined using a Dual-Luciferase reporter assay system (Promega) according to the directions provided by the manufacturer.

RT-PCR. Total RNA was extracted from the cultured cells and various mouse tissues using Trizol reagent (Invitrogen). Reverse-transcription (RT) for synthesizing the first-strand cDNAs was carried out using oligo(dT) primer and SuperScript II reverse transcriptase (Invitrogen) according to the manufacturer's instructions, and the resultant cDNAs were examined by real-time PCR using the ABI PRISM 7000 sequence detection system (Applied Biosystems) with a SYBER Green PCR Master Mix or a TaqMan Universal PCR Master Mix together with Assays-on-Demand Gene Expression products (Applied Biosystems) according to the manufacturer's instructions. For plotting a standard curve, the 1, 5, 25, 125, and 625-fold diluted brain cDNA samples, which were prepared from a brain tissue (total RNA) and designated as standards, were used in every real-time PCR. Expression levels of the genes examined were normalised to that of the control *G3pdh* gene. The PCR primers used in the real-time PCR were as follows:

G3pdh-F; 5′-TCTTCACCACCATGGAGAAG-3′
G3pdh-R; 5′-TCATGGATGACCTTGGCCAG-3′
Dicer-F; 5′-GCAGGCTTTTACACACGCCT-3′
Dicer-R; 5′-GGGTCTTCATAAAGGTGCTT-3′
eIF2C2-F; 5′-AGATGAAGAGGAAGTACCGT-3′
eIF2C2-R; 5′-CAGAACCAGCTTGTGCCTGT-3′

The Assays-on-Demand Gene Expression products used (the Assay ID numbers) were as follows:

eIF2C1; Mm00462977m1, *eIF2C3*; Mm00462959m1, *eIF2C4*; Mm00462659m1.

5-Bromodeoxyuridine incorporation assay. Cells were metabolically labeled in the culture medium containing 10 μM of 5-bromodeoxyuridine (BrdU) (Sigma) for 20 h, and rinsed with phosphate-buffered saline solution (PBS) followed by fixation with 70% ethanol containing 0.5 M HCl at −20 °C for 1 h. The resultant cells were incubated with anti-BrdU antibody (Oxford biotechnology) at 4 °C overnight. The BrdU-antibody complexes were visualised with Alexa488 conjugated secondary antibody (Invitrogen) and examined using a ZEISS (Axiovert) microscope.

Results and discussion

Expression profiles of Dicer and eIF2C1∼4 in various mouse tissues

Previous studies suggested that *Dicer* and *eIF2C* translation initiation factors (*eIF2C1∼4*) homologous to the *Ago* genes in *Drosophila* [26,27] contributed to mammalian RNAi [21,22]. *Dicer* appears to be expressed ubiquitously, but its expression level varies among tissues [16,17]. Since little is known about the expression levels of *eIF2C1∼4* among tissues, we first examined the levels of expression of *eIF2C1∼4* and *Dicer* in various tissues. Total RNA was extracted from mouse tissues and subjected to cDNA synthesis with oligo(dT) primer and reverse transcriptase. The resultant cDNAs were examined by a real-time PCR. The results are shown in Fig. 1. The expression level of *Dicer* in either skeletal muscle or heart appears to be lower than those in other tissues, which agrees with the previous observations [16,17]. It should be noted that the expression levels of *eIF2C1∼4* in either skeletal muscle or heart, like the expression profile of *Dicer*, are also significantly lower than those in the other tissues examined. Consequently, the observations suggest that

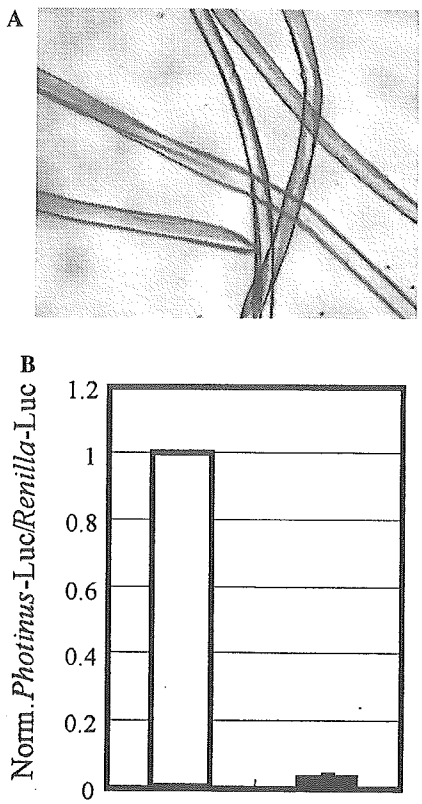

Fig. 2. RNAi induction by synthetic siRNA duplexes in muscle fibers prepared from mouse extensor digitorum longus. (A) Photograph of isolated muscle fibers. Isolation of muscle fibers from mouse extensor digitorum longus was carried out as described in Materials and methods. (B) RNAi activity in isolated muscle fibers. The La2 siRNA duplex against the *Photinus* luciferase gene [25] or a non-silencing siRNA duplex (Qiagen) together with pGL3-control and pRL-SV40 plasmids carrying *Photinus* and *Renilla* luciferase reporter genes, respectively, were cotransfected into the isolated muscle fibers. Twenty-four hours after transfection, cell lysate was prepared and dual luciferase assay was carried out. Ratios of normalised target (*Photinus*) luciferase activity to control (*Renilla*) luciferase activity are indicated: the ratios of luciferase activity determined in the presence of the La2 siRNA duplex are normalised to the ratios obtained in the presence of the non-silencing siRNA duplex. Open and solid bars indicate the data in the presence of the non-silencing siRNA and La2 siRNA duplexes, respectively. Data are averages of at least three independent experiments. Error bars represent standard deviations.

skeletal and cardiac muscle cells express either *Dicer* or *eIF2C1~4* at a low level.

RNAi activity in muscle fibers isolated from mouse extensor digitorum longus

The observations described above raised the question whether RNAi could occur in muscle, i.e., whether RNAi could be induced under a condition with a low level of expression of either *Dicer* or *eIF2C1~4*. In order to address the question, we isolated mouse muscle fibers from extensor digitorum longus of ICR mice (Fig. 2A), and introduced synthetic 21-nt siRNA duplex targeting the exogenous reporter gene, *Photinus* luciferase, together with a pGL3-control plasmid carrying the *Photinus luciferase* gene and a pRL-SV40 plasmid carrying the *Renilla luciferase* gene as a control into the isolated muscle fibers. For realizing an efficient RNAi induction, we used the La2 siRNA duplex having the potential for inducing a strong RNAi activity in cultured mammalian cells [25]. As shown in Fig. 2B, the results indicate that the La2 siRNA duplex can induce a strong gene silencing of the *Photinus luciferase* gene in the muscle fibers. This result suggests that RNAi can be induced by synthetic siRNA duplexes in skeletal muscle which barely expresses either *Dicer* or *eIF2C1~4*.

RNAi activity during myogenic differentiation of mouse C2C12 cells

To further examine the properties of RNAi in muscle cells and during myogenic differentiation, we investigated RNAi activity in C2C12 cells, a mouse myoblast cell line, which can be induced by changing culture conditions (detailed in Materials and methods) to differentiate into contractile myotubes [24]. First, we

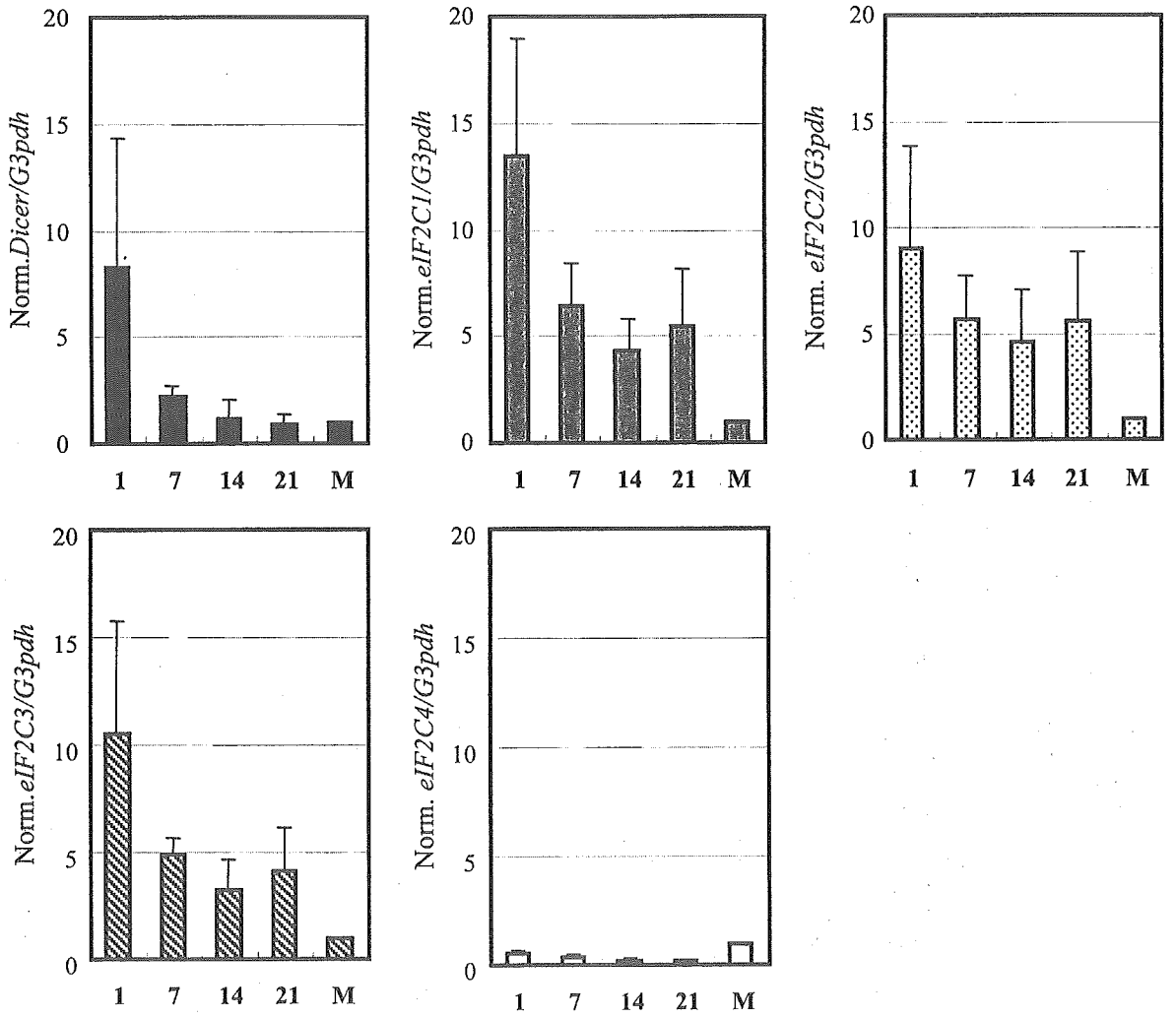

Fig. 3. Expression profiles of *Dicer* and *eIF2C1~4* during myogenic differentiation of mouse C2C12 cells. Total RNA was extracted from C2C12 cells at various days (indicated) after induction of myogenic differentiation of the cells (day 1 indicates undifferentiated C2C12 cells), and subjected to RT-PCR to examine the expression levels of *Dicer* and *eIF2C1~4* as in Fig. 1. The expression levels of the genes are normalised and plotted as in Fig. 1. M indicates skeletal muscle. Data are averages of three independent experiments. Error bars represent standard deviations.

examined the expression profiles of *Dicer* and *eIF2C1~4* during the myogenic differentiation of C2C12 cells and compared them with those of skeletal muscle examined above. As shown in Fig. 3, the expression profiles reveal that the level of expression of either *Dicer* or *eIF2C1~3* is gradually decreased during the myogenic differentiation of C2C12 cells, and that the *eIF2C4* gene is expressed at a low level in either C2C12 myoblast or myotube.

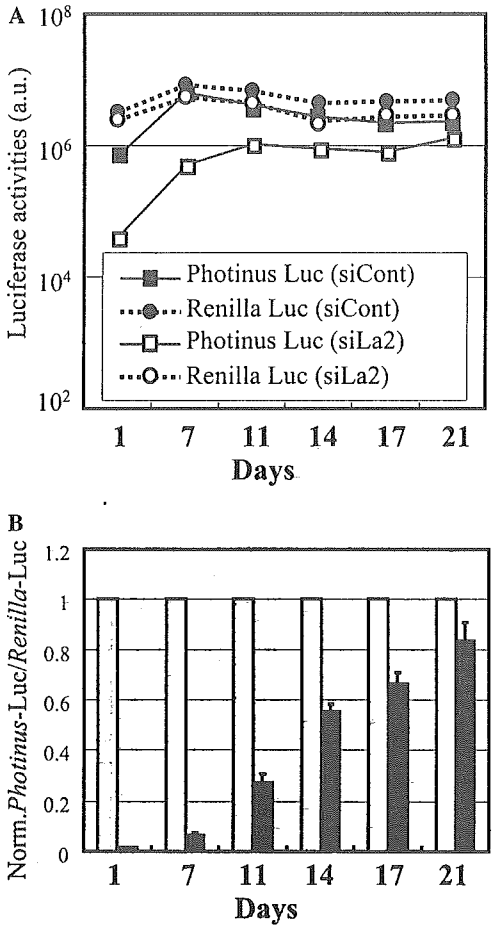

Fig. 4. Persistence of RNAi activity during myogenic differentiation of mouse C2C12 cells. The La2 siRNA duplex or a non-silencing siRNA duplex (Qiagen) together with pGL3-control and pRL-SV40 plasmids were cotransfected into C2C12 cells as in Fig. 2. Before transfection, the culture medium (DMEM containing 15% fetal calf serum) was replaced with DMEM containing 5% horse serum for induction of the myogenic differentiation of C2C12 cells. RNAi activity was examined 24 h after transfection (day 1), and thereafter examined at various days (indicated) up to 3 weeks after the transfection. (A) Absolute *Photinus* and *Renilla* luciferase expressions. The expression levels are plotted in arbitrary luminescence units (a.u.). (B) Ratios of normalised target to control luciferase. Ratios of normalised target (*Photinus*) luciferase activity to control (*Renilla*) luciferase activity are indicated as in Fig. 2. Open and solid bars indicate the data in the presence of the non-silencing siRNA and La2 siRNA duplexes, respectively. Data are averages of at least three independent experiments. Error bars represent standard deviations.

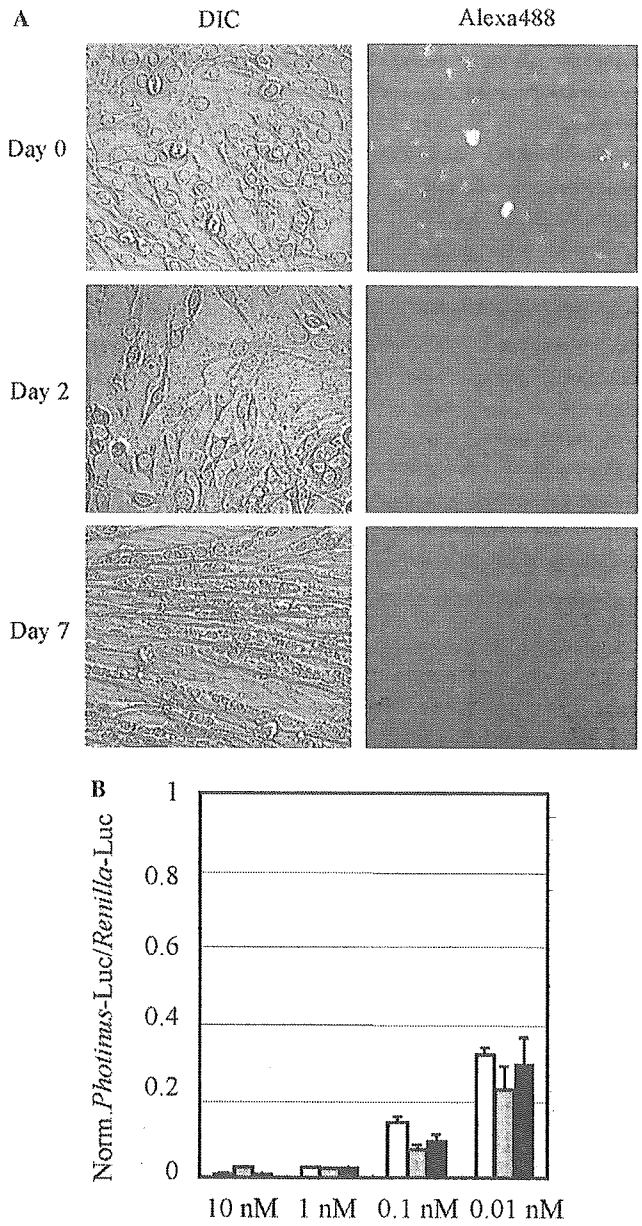

Fig. 5. Cell-cycle arrest and RNAi activity during myogenic differentiation of C2C12 cells. Myogenic differentiation of C2C12 cells was induced by changing the culture medium from DMEM containing 15% fetal calf serum to DMEM containing 5% horse serum. (A) Cell-cycle arrested C2C12 cells. Metabolically labeling of the cells with BrdU was carried out at indicated days after the differentiation. Day 0 indicates undifferentiated C2C12 cells. BrdU incorporated into the cells was visualised with an anti-BrdU antibody and an Alexa488 conjugated secondary antibody. The cells were examined by a florescent microscope. Left (DIC, differential interference contrast) and right (Alexa488, florescence image) panels are identical in visual field. (B) RNAi activity during the differentiation. The reporter plasmids carrying the *Photinus* and *Renilla luciferase* genes were cotransfected with a decreasing amount of the La2 siRNA or non-silencing siRNA duplexes (Qiagen), from 10 to 0.01 nM, into either undifferentiated or differentiated C2C12 cells. Ratios of normalised target (*Photinus*) luciferase activity to control (*Renilla*) luciferase activity are indicated as in Fig. 2. Open, dotted, and solid bars indicate the data in C2C12 cells that differentiated for 0 (undifferentiated), 2, and 7 days, respectively. Data are averages of at least three independent experiments. Error bars represent standard deviations.

Next we examined RNAi activity during the myogenic differentiation of C2C12 cells. The La2 siRNA duplex together with pGL3-control and pRL-SV40 plasmids was cotransfected into undifferentiated C2C12 cells, and simultaneously myogenic differentiation of the cells was carried out by changing culture medium as described above (see Materials and methods). As a result, a strong RNAi activity was detected by day 7 after RNAi induction (Fig. 4), when morphological changes of C2C12 cells into myotubes appeared to be completed (Fig. 5A); thereafter, the cells gradually lost the RNAi activity and lost most of the activity by day 21 after the induction (Fig. 4).

Because proliferating mammalian cells gradually lose RNAi activity with an increase in the number of cell divisions [12,28,29], we investigated whether cell division occurred in C2C12 cells during the differentiation by means of a BrdU incorporation assay. As shown in Fig. 5A, while the incorporation of BrdU into nuclei could be observed in undifferentiated C2C12 cells, few or no BrdU-positive cells were detectable at day 2 and 7 after induction of the differentiation. In addition, from the data of Fig. 5B, the nature of RNAi activity during the differentiation appears to remain unchanged. Consequently, these observations suggest that C2C12 cells differentiated over 2 days are probably cell-cycle arrested cells, and thus that the decrease in RNAi activity during the myogenic differentiation of C2C12 cells is not caused by cell division.

We further examined RNAi activities in C2C12 myotubes that differentiated for 14 and 21 days. The results indicate that RNAi activities induced by synthetic siRNA duplexes are detectable in those differentiated C2C12 myotubes (Fig. 6), although the transfection efficiency of siRNA and plasmid DNA into the cells seemed to become lower as the culture was long. Taking all the data together, it is conceivable that the decrease in RNAi activity during the myogenic

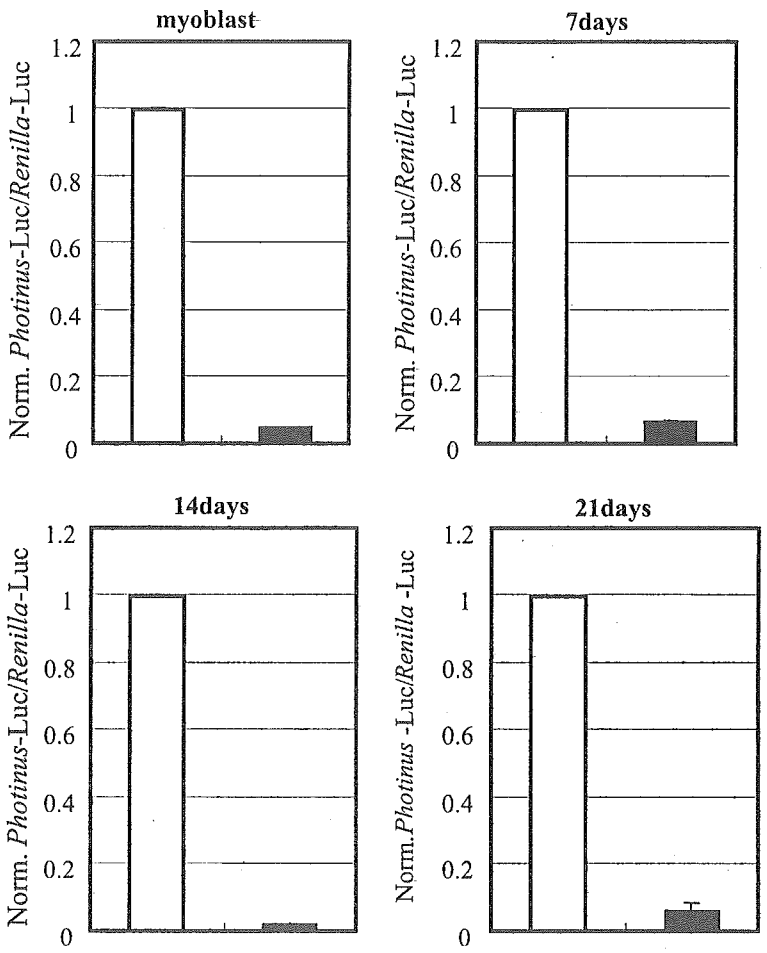

Fig. 6. RNAi induction after myogenic differentiation of C2C12 cells. Myogenic differentiation of C2C12 cells was performed as in Fig. 5. RNAi induction was carried out as in Fig. 2 at indicated days after induction of the myogenic differentiation, and each RNAi activity was examined 24 h after RNAi induction. Ratios of normalised target (*Photinus*) luciferase activity to control (*Renilla*) luciferase activity are indicated as in Fig. 2. Open and solid bars indicate the data in the presence of the non-silencing siRNA and La2 siRNA duplexes, respectively. Data are averages of at least three independent experiments. Error bars represent standard deviations.

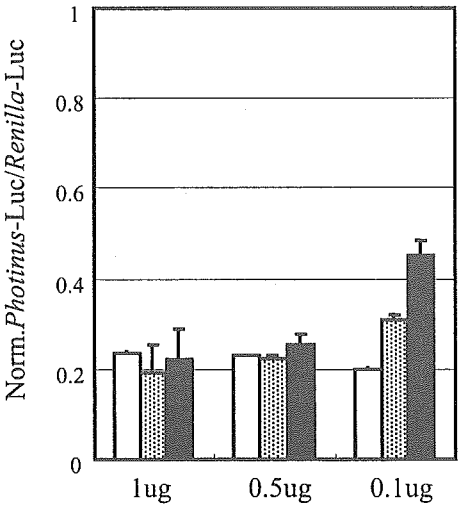

Fig. 7. RNAi induction by short-hairpin RNAs during myogenic differentiation of C2C12 cells. The pRNA-U6.1/Neo/siFluc plasmid (GenScript), which can express a short-hairpin RNA (shRNA) against *Photinus luciferase*, and pRNA-U6.1/Neo empty vector (GenScript) as a control were used. The pGL3-control and phRL-TK plasmids together with a decreasing amount of each of the pRNA-U6.1/Neo/siFluc and pRNA-U6.1/Neo (a negative control) plasmids, from 1 to 0.1 μg, were cotransfected into C2C12 cells. The expression of luciferase was examined 24 h after the transfection. Ratios of normalised target (*Photinus*) luciferase activity to control (*Renilla*) luciferase activity are indicated as in Fig. 2. Open, dotted, and solid bars indicate the data in C2C12 cells that differentiated for 0 (undifferentiated), 2, and 7 days, respectively. Data are averages of at least three independent experiments. Error bars represent standard deviations.

differentiation of C2C12 cell may be caused by losing the stability of functional RISCs in the differentiated C2C12 myotubes.

RNAi induction by short-hairpin RNAs in C2C12 cells

Because Dicer appears to be required for the process of short-hairpin RNAs (shRNAs) into siRNA duplexes, it may be of interest to see if shRNAs can induce RNAi in C2C12 myotubes which barely express *Dicer*. To examine this, we introduced a shRNA expression plasmid against *Photinus* luciferase, pRNA-U6.1/Neo/siRNA, together with the reporter plasmids carrying the *Photinus* and *Renilla* luciferase genes into C2C12 myoblast and myotubes. The results indicate that the shRNA expression plasmid, or shRNAs can induce RNAi in either C2C12 myoblast or myotube (Fig. 7), suggesting that the Dicer protein could be present in those cells. An interesting point to note is that a decrease in the RNAi activity induced by 0.1 μg pRNA-U6.1/Neo/siRNA was observed in C2C12 myotubes that differentiated for 7 days. This may be caused by a possible decrease in the amounts of Dicer and eIF2C1~4 in the cells. To further evaluate the results and a possible relationship between the quantitative level of either Dicer or eIF2C1~4 and RNAi activity, more extensive studies must be conducted.

Integrity of mammalian RNAi

Our previous study has demonstrated that RNAi activity induced by synthetic siRNA duplexes in post mitotic neurons persists for at least 3 weeks, i.e., a long-lasting RNAi activity occurs in mammalian neurons [29]. Our present and previous studies, therefore, suggest that there is a significant difference in the duration of RNAi activity between muscle and neuron, both of which are terminally differentiated and cell cycle-arrested cells. Since neither muscle nor neuron probably undergoes a decrease in the number of functional RISCs by cell division, it may be possible that the stability of functional RISCs could differ between muscle and neuron.

The present observations further suggest the possibility that a little amount of either Dicer or eIF2C1~4 might be sufficient for activation of mammalian RNAi. This seems to be an important point for understanding mammalian RNAi, and further studies on the contribution of either Dicer or eIF2C1~4 to mammalian RNAi must be conducted.

Finally, all the data presented here lead us to the possibility that RNAi may be applicable for a creation of possible model cells and/or model animals for inherited muscular diseases, for example, muscular dystrophy.

Acknowledgments

We thank Drs. Ojima and Takeda (National Institute of Neuroscience) for their technical advice on the preparation of muscle fibers from mouse extensor digitorum longus. This work was supported in part by a Grant-in-Aid from the Japan Society for the Promotion of Science and by research grants from the Ministry of Health, Labor and Welfare in Japan.

References

[1] P.A. Sharp, RNAi and double-strand RNA, Genes Dev. 13 (1999) 139–141.
[2] J.M. Bosher, M. Labouesse, RNA interference: genetic wand and genetic watchdog, Nat. Cell Biol. 2 (2000) E31–E36.
[3] H. Vaucheret, C. Beclin, M. Fagard, Post-transcriptional gene silencing in plants, J. Cell Sci. 114 (2001) 3083–3091.
[4] H. Cerutti, RNA interference: traveling in the cell and gaining functions?, Trends Genet. 19 (2003) 39–46.
[5] S.M. Hammond, E. Bernstein, D. Beach, G.J. Hannon, An RNA-directed nuclease mediates post-transcriptional gene silencing in *Drosophila* cells, Nature 404 (2000) 293–296.
[6] P.D. Zamore, T. Tuschl, P.A. Sharp, D.P. Bartel, RNAi: double-stranded RNA directs the ATP-dependent cleavage of mRNA at 21 to 23 nucleotide intervals, Cell 101 (2000) 25–33.
[7] E. Bernstein, A.A. Caudy, S.M. Hammond, G.J. Hannon, Role for a bidentate ribonuclease in the initiation step of RNA interference, Nature 409 (2001) 363–366.
[8] S.M. Elbashir, W. Lendeckel, T. Tuschl, RNA interference is mediated by 21- and 22-nucleotide RNAs, Genes Dev. 15 (2001) 188–200.